

IMPROVED LABORATORY TRANSITION PROBABILITIES FOR Nd II AND APPLICATION TO THE NEODYMIUM ABUNDANCES OF THE SUN AND THREE METAL-POOR STARS

E. A. DEN HARTOG AND J. E. LAWLER

Department of Physics, University of Wisconsin, Madison, WI 53706; eadener@wisc.edu, jelawler@wisc.edu

C. SNEDEN

Department of Astronomy and McDonald Observatory, University of Texas, Austin, TX 78712; chris@verdi.as.utexas.edu

AND

J. J. COWAN

Department of Physics and Astronomy, University of Oklahoma, Norman, OK 73019; cowan@nhn.ou.edu

Received 2003 April 18; accepted 2003 May 13

ABSTRACT

Radiative lifetimes, accurate to $\pm 5\%$, have been measured for 168 odd-parity levels of Nd II using laser-induced fluorescence. The lifetimes are combined with branching fractions measured using Fourier-transform spectrometry to determine transition probabilities for over 700 lines of Nd II. This work is the largest-scale laboratory study to date of Nd II transition probabilities using modern methods. This improved data set is used to determine Nd abundances for the Sun and three metal-poor giant stars with neutron-capture enhancement: CS 22892–052, HD 115444, and BD +17°3248. In all four stars the line-to-line scatter is considerably reduced from earlier published results. The solar photospheric abundance is determined to be $\log \epsilon(\text{Nd}) = 1.45 \pm 0.01 (\sigma = 0.05)$, which is in excellent agreement with meteoric data. The ratio of Nd/Eu is virtually identical in all three metal-poor Galactic halo stars. Furthermore, the newly determined stellar Nd abundances, in comparison with other heavy neutron-capture elements, are consistent with an *r*-process-only origin early in the history of the Galaxy. These more accurate Nd abundance determinations might help to constrain the predicted solar system *r*-process abundances, and suggest other elements for further neutron-capture abundance studies.

Subject headings: atomic data — stars: abundances — Sun: abundances

On-line material: machine-readable tables

1. INTRODUCTION

High-resolution, high signal-to-noise ratio (S/N) spectra from very large ground-based telescopes and the *Hubble Space Telescope* are providing data that are reshaping our views on the chemical evolution of our Galaxy. Recent abundance determinations of heavy neutron capture (*n*-capture) elements in very metal poor stars have yielded new insights on the roles of the *r*(apid)- and *s*(low)-processes in the initial burst of Galactic nucleosynthesis. Substantial progress is occurring as a result of improvements in both observational data and laboratory data needed for analysis of the spectra.

The rare earths are among the most spectroscopically accessible of the *n*-capture elements. Large numbers of ionized-species transitions of rare earths appear in the spectrum of the Sun and in stars over a significant temperature range. Motivation for the present study of Nd has arisen from studies of metal-poor Galactic halo stars. The richness of Nd II, with thousands of known spectral lines connected to low levels, has delayed progress on this spectrum until now. While Nd II has many convenient lines for analysis, stellar spectroscopists have known that the transition probability database has been lacking in absolute accuracy and in scope. The resulting Nd abundance determinations from older sets of transition probabilities exhibit large line-to-line scatter, which causes concern about overall accuracy.

The current work on Nd II represents a continuation of a series of studies aimed at improving the transition parameters for rare earth species, and thereby refining the abundance determinations for those species. In recent years our

group has completed studies of Lu II (Den Hartog et al. 1998; Fedchak et al. 2000), La II (Lawler, Bonvallet, & Sneden 2001a), Tb II (Den Hartog, Fedchak, & Lawler 2001; Lawler et al. 2001b), and Eu II (Lawler et al. 2001c). The solar abundances of several of these elements have been brought into agreement with meteoric abundances through improvements in the transition probability database (see, e.g., Bord, Cowley, & Mirjianian 1998; Den Hartog et al. 1998; Lawler et al. 2001b).

The above-mentioned studies on La II, Tb II, and Eu II included measurements of both transition probabilities and hyperfine structure data. Lines of Nd II are, with few exceptions, rather narrow, with no resolved structure on our spectra with resolving powers up to 10^7 . Hence, new hyperfine data are not currently needed for astrophysical studies, and the laboratory work reported here emphasizes only improved transition probabilities. In the present study, we have measured radiative lifetimes using time-resolved laser-induced fluorescence for 168 odd-parity levels of Nd II. These are combined with branching fractions measured using Fourier-transform spectrometry to yield *gf*-values for over 700 transitions of Nd II. This new data set is used to reanalyze the photospheric abundances of four stars: the Sun and three metal-poor halo stars, CS 22892–052, HD 115444, and BD +17°3248.

2. RADIATIVE LIFETIME MEASUREMENTS

Radiative lifetimes of 168 odd-parity levels of Nd II have been measured at the University of Wisconsin. The lifetimes are measured using time-resolved laser-induced

fluorescence (LIF) on a slow atom/ion beam. The apparatus and technique are the same as used for lifetime measurements in numerous other species, and only an abbreviated description will be given here. The reader is referred to recent work in Eu I, II, and III and Tb II (Den Hartog, Wickliffe, & Lawler 2002; Den Hartog et al. 2001) for a more in-depth discussion.

The beam of Nd atoms and ions is produced using a large-bore hollow cathode discharge (HCD) sputter source, operating at ~ 0.3 torr argon pressure with ~ 40 mA DC and ~ 10 A, $10\ \mu\text{s}$ duration current pulses. This source produces a slow ($\sim 5 \times 10^4\ \text{cm s}^{-1}$), weakly collimated beam, which is extracted into a low-pressure (10^{-4} torr) scattering chamber. Tests performed over the years have shown that the low background pressure, low-density beam environment results in measurements free from collisional quenching and radiation trapping. The beam contains both neutral and singly ionized Nd in the ground state or low-lying metastable levels. For Nd ions, of interest in this work, metastables up to $\sim 10,000\ \text{cm}^{-1}$ are sufficiently populated in the beam to be useful as lower levels for the laser excitation.

The ion beam is crossed at right angles with a beam from a nitrogen laser pumped dye laser. The dye laser is tunable over the range 205–720 nm with the use of frequency-doubling crystals, has a pulse length of ~ 3 ns, and a bandwidth of $0.2\ \text{cm}^{-1}$. The narrow bandwidth of the laser allows the selective excitation of the level to be studied. The resulting fluorescence is collected in a direction mutually orthogonal to both beams, through a pair of fused silica lenses comprising an f/1 optical system. Optical filters are often inserted between the two lenses in order to block laser light scattered from windows or other surfaces and to block cascade radiation from lower levels. There is no possibility of cascade from higher levels because of the selective nature of the laser excitation.

The fluorescence is detected with a RCA 1P28A photomultiplier tube (PMT) and a decay curve is recorded using a Tektronix SCD1000 digitizer. The laser is then tuned off the transition and a background trace is recorded. A linear least-square fit to a single exponential is performed on the background-subtracted decay to yield the lifetime of the excited level. The lifetime of each level is measured at least twice, using different laser transitions for excitation whenever possible. This duplication helps ensure that the transitions are identified correctly in the experiment, are free from blends, and are classified correctly to the upper level being studied.

The dynamic range of the experiment is from 2 ns to $\sim 1.5\ \mu\text{s}$. The bandwidth of the electronics limits the shortest lifetime measurable to 2 ns, while the limit on the long end of the range is due to ions leaving the viewing region before radiating. The ion motion causes an apparent shortening of the measured lifetime, because ions fluorescing late in the decay are more likely to have left the viewing region than ions fluorescing earlier. For ion lifetimes longer than ~ 100 ns, a third lens is inserted into the fluorescence collection system. This lens effectively defocuses the image at the PMT, making the system less sensitive to motion of the ions. The longest lifetimes reported in this study ($\tau < 300$ ns) are short enough that no further correction is required to adjust for the motion of the ions.

The fluorescence decay curve may also be distorted by Zeeman quantum beats (Corney 1977). These beats occur when the polarized laser produces dipole-aligned ions,

which subsequently precess about the earth's magnetic field as they radiate. The anisotropic radiation patterns rotate through the viewing direction resulting in an oscillation of the observed fluorescence. Zeeman beats can be controlled by zeroing the magnetic field in the center of the scattering chamber with Helmholtz-like coils. The field is zeroed to within $\pm 20\ \text{mG}$ for short lifetimes. For long lifetimes, a high field of 30 G is maintained in the chamber, resulting in very rapid oscillations which average to zero on the timescales comparable to the lifetime.

With only one exception, the lifetimes we report have an uncertainty of $\pm 5\%$. In order to maintain this level of fidelity over the full dynamic range and from one set of measurements to another, we perform periodic end-to-end tests of the experiment. We measure a set of well-known lifetimes, or in some cases ratios of lifetimes, to which we can compare our results. These cross-checks are discussed in detail in Den Hartog et al. (2002). They include lifetimes for levels in Be I (Weiss 1995), Be II (Yan, Tambasco, & Drake 1998), and Fe II (Guo et al. 1992; Biémont et al. 1991), covering the range 1.8–8.8 ns. He I lifetimes are measured in the range 95–220 ns (Kono & Hattori 1984). In addition, relative absorption oscillator strengths of Cr I (Blackwell, Menon, & Petford 1984) and Fe I (Blackwell et al. 1979a; Blackwell, Petford, & Shallis 1979b) are used to calculate accurate ratios of lifetimes. These ratios help fill in the gap between 9 and 95 ns, where there are no convenient benchmark lifetimes to measure. The Cr I lifetime ratio ties together the lifetimes around 30 ns to those at 6 ns. The Fe I lifetime ratios tie together lifetimes near 6, 60, and 90 ns.

Our results of lifetime measurements of 168 odd-parity levels of Nd II are given in Table 1. Energy levels are taken from Blaise et al. (1984), with additional levels from Martin, Zalubas, & Hagan (1978). Air wavelengths are calculated from the energy levels using the standard index of air (Edlén 1953, 1966). The uncertainty of the lifetimes is $\pm 5\%$, with one exception, which is noted in the table.

A comparison of our results to other lifetimes available in the literature is shown in Table 2. We see very good agreement with the laser-fast beam measurements of Ward et al. (1985). The mean difference between our measurements and theirs is $+1.8\%$, and the rms difference is 6.4% when the serious discordance at $27445\ \text{cm}^{-1}$ is omitted. No obvious reason for this single discordance can be found. Our lifetime for this level is the result of two separate measurements using different laser excitation transitions and careful optical filtering, so our confidence in the lifetime is high. The single laser-fast beam measurement of Wei et al. (1991) on the $23537\ \text{cm}^{-1}$ level is 8% longer than our lifetime. We are, however, in excellent agreement with Ward et al. (1985) on that level. Agreement with the non-LIF measurements reported in the literature is not as good. The delayed coincidence measurements of Gorshkov et al. (1982) show mean and rms differences of $+33\%$ and 56% , respectively, when compared to our measurements. The mean and rms differences between the beam foil measurements of Andersen et al. (1975) and ours are $+47\%$ and 81% , respectively. This poor agreement is likely due to the difficulty of removing cascade contributions from higher lying levels in these techniques which utilize nonselective excitation processes. The excellent agreement between independent LIF lifetime measurements in Nd II and in many other spectra now provides additional confidence that absolute scales for transition probabilities in these spectra are reliable.

TABLE 1
LIFETIMES OF ODD-PARITY LEVELS IN Nd II

Energy ^a (cm ⁻¹)	J	Laser Wavelength in Air ^b (nm)	Lifetime (ns)
20672.57.....	4.5	495.912, 525.551	79.6
20830.03.....	3.5	492.069, 521.236	63.5
20907.32.....	5.5	490.204, 514.334, 519.144	137
21241.07.....	2.5	470.654	77.7
21291.74.....	3.5	481.134, 508.983	95.5
21871.51.....	3.5	468.074, 494.390	196
21918.05.....	4.5	467.056, 488.910	123
22187.65.....	4.5	482.548, 522.842	62.9
22358.06.....	4.5	447.140, 478.611	271
22389.84.....	3.5	446.506, 482.034	139
22455.62.....	4.5	445.198, 455.613	107
22578.16.....	6.5	500.043, 512.378	136
22663.71.....	4.5	451.333, 471.708	209
22696.87.....	5.5	450.658, 509.279	77.2
22850.54.....	3.5	447.558, 471.559	84.1
23159.97.....	5.5	441.443, 485.903	76.8
23171.11.....	4.5	431.451, 441.226	119
23229.98.....	4.5	430.357, 531.981	12.5
23378.31.....	5.5	437.227, 456.322	174
23397.37.....	3.5	427.278, 459.701	63.3
23409.52.....	4.5	427.057, 459.445	67.1
23458.95.....	5.5	458.403, 478.943	176
23537.38.....	4.5	424.737, 523.419	25.6
23771.03.....	4.5	420.562, 482.857	235
23857.26.....	5.5	446.559, 450.181	68.4
23991.40.....	6.5	443.899, 513.233	161
24053.34.....	4.5	415.625, 446.241	73.0
24134.08.....	5.5	423.237, 444.638	23.4
24243.21.....	6.5	489.069, 506.683	97.1
24321.24.....	4.5	411.047, 437.492	52.1
24445.38.....	5.5	417.732, 435.128	15.1
24468.03.....	3.5	408.581, 417.337	168
24569.77.....	4.5	406.889, 436.186	282
24721.04.....	6.5	429.969, 451.635	121
24842.87.....	5.5	410.907, 516.513	30.3
24913.85.....	3.5	401.270, 429.734	54.9
25014.91.....	5.5	408.022, 445.717	130
25044.64.....	3.5	399.174, 407.527	19.9
25080.86.....	5.5	406.926, 423.417	40.4
25138.55.....	3.5	397.683, 425.623	34.7
25200.90.....	5.5	424.496, 483.227	96.4
25295.28.....	3.5	395.219, 422.802	29.8
25352.37.....	5.5	402.478, 418.603	59.4
25389.21.....	4.5	401.882, 417.958	36.2
25394.62.....	6.5	417.864, 462.990	159
25481.27.....	5.5	400.400, 436.639	49.9
25524.47.....	6.5	415.608, 529.316	8.4
25771.52.....	4.5	395.799, 411.383	39.2
25876.54.....	2.5	386.341, 582.586	11.9
25877.16.....	4.5	386.332, 394.151	14.1
26031.47.....	7.5	464.576, 498.716	98.7
26041.20.....	2.5	383.898, 577.049	20.8
26116.03.....	2.5	382.798	90.5
26182.48.....	5.5	389.462, 407.511	39.3
26206.80.....	3.5	381.472, 389.094	17.0
26210.74.....	6.5	404.079, 510.757	18.2
26227.09.....	4.5	381.177, 388.787	48.3
26274.09.....	5.5	388.077, 405.995	18.6
26292.50.....	3.5	380.229	134
26328.02.....	6.5	402.173, 429.778	43.5
26369.05.....	3.5	386.652, 404.435	104
26380.73.....	4.5	401.322	145
26422.54.....	3.5	385.854	146
26500.40.....	4.5	384.698, 402.298	193

TABLE 1—Continued

Energy ^a (cm ⁻¹)	J	Laser Wavelength in Air ^b (nm)	Lifetime (ns)
26640.08.....	3.5	382.641, 400.049	20.8
26670.59.....	4.5	396.706	155
26738.79.....	6.5	422.320, 449.791	139
26759.22.....	4.5	380.904, 421.956	84.5
26761.10.....	5.5	380.877, 395.286	34.1
26772.08.....	5.5	397.947, 413.335	11.2
26793.33.....	3.5	380.410, 397.611	117
26912.77.....	7.5	410.945, 446.298	7.1
26926.99.....	4.5	378.484, 392.710	47.6
26991.89.....	5.5	409.612	89.9
27014.27.....	4.5	377.238, 391.368	144
27146.56.....	6.5	428.244, 472.436	40.3
27179.60.....	4.5	367.818, 374.899, 391.594	78.0
27233.53.....	4.5	388.037, 390.769	30.9
27245.45.....	5.5	387.858, 413.471	22.3
27308.95.....	6.5	386.905, 404.359	30.6
27352.29.....	5.5	386.257, 388.963	55.0
27425.00.....	4.5	385.175, 410.423	27.2
27444.53.....	3.5	387.572	103
27445.85.....	7.5	402.133, 435.924	32.9
27448.71.....	6.5	402.086, 422.771	15.6
27504.11.....	3.5	386.679	131
27518.40.....	5.5	383.793, 408.855	76.8
27553.50.....	4.5	383.277, 385.942	119
27611.72.....	7.5	399.467, 432.793	20.8
27694.62.....	3.5	360.978, 383.851	68.9
27721.43.....	6.5	380.825, 405.488	122
27744.19.....	6.5	397.364, 405.114	20.4
27769.43.....	5.5	380.130, 396.966	122
27781.76.....	5.5	379.952, 396.771	109
27805.38.....	3.5	359.540, 366.303	156
27816.79.....	7.5	396.220, 457.931	55.8
27921.38.....	4.5	377.946	15.2
27934.52.....	4.5	364.578, 380.347	37.4
27990.04.....	4.5	379.545	69.8
27992.43.....	5.5	393.481, 425.776	46.4
27993.23.....	8.5	436.414, 454.260	57.3
28089.47.....	6.5	375.560, 399.524	62.3
28170.45.....	4.5	376.963, 398.235	44.3
28196.15.....	6.5	390.351, 409.817	74.9
28213.87.....	3.5	354.334, 376.347	28.9
28285.61.....	5.5	388.993, 396.417	16.4
28298.46.....	4.5	359.802	101
28340.55.....	4.5	352.750, 359.258	90.1
28354.40.....	6.5	387.954, 446.925	27.0
28418.97.....	8.5	406.108, 428.451	6.9
28540.95.....	7.5	385.166, 404.106	28.4
28563.48.....	6.5	392.096, 403.738	16.5
28582.62.....	5.5	356.160, 368.728	98.3
28725.93.....	6.5	389.614, 401.106	71.7
28729.74.....	7.5	401.045, 439.550	98.7
28748.53.....	8.5	400.743, 422.484	58.2
28856.89.....	7.5	380.534, 420.558	12.9
28860.16.....	5.5	367.408, 387.586	45.3
28899.07.....	6.5	379.924, 398.339	93.7
28926.24.....	4.5	366.518, 386.596	56.5
29027.54.....	8.5	396.310, 417.560	11.4
29036.65.....	3.5	365.040	176
29043.45.....	4.5	384.851, 452.124	25.0
29088.72.....	6.5	395.351	43.4
29239.38.....	5.5	375.073, 381.970	89.9
29260.74.....	7.5	403.955, 413.532	35.3
29298.63.....	4.5	361.581, 381.107	53.7
29336.73.....	5.5	358.750, 380.555	28.6
29362.52.....	7.5	391.117, 521.565	12.6

TABLE 1—Continued

Energy ^a (cm ⁻¹)	J	Laser Wavelength in Air ^b (nm)	Lifetime (ns)
29434.26.....	6.5	390.022, 426.343	14.0
29484.61.....	5.5	378.424	13.5
29701.47.....	6.5	396.887	80.7
29864.64.....	4.5	373.058	60.8
29955.41.....	7.5	392.925, 401.981	46.8
30002.31.....	9.5	401.224, 513.059	5.4
30037.08.....	2.5	332.826	49.2
30094.85.....	7.5	390.784, 399.740	36.0
30246.77.....	8.5	378.038, 397.326	12.1
30306.15.....	7.5	396.391	59.6
30348.34.....	6.5	360.090, 376.592	107
30405.58.....	7.5	386.094, 394.834	34.1
30431.85.....	2.5	328.508	101
30453.34.....	3.5	328.277, 333.905	68.5
30467.35.....	6.5	374.911	29.1
30570.21.....	6.5	363.487, 383.655	37.7
30659.82.....	2.5	326.066	150
30691.07.....	5.5	361.897	62.6
30700.78.....	6.5	355.576	104
30707.28.....	7.5	371.568, 390.185	15.9
30781.49.....	8.5	389.058, 403.178	10.3
30813.11.....	6.5	354.161, 380.111	53.5
31153.86.....	6.5	365.501, 375.250	29.4
31179.76.....	4.5	336.494	112
31186.58.....	3.5	325.923	110
31256.77.....	6.5	373.806, 395.596	21.4
31274.81.....	5.5	373.554	36.5
31362.12.....	7.5	362.739, 393.953	133
31451.30.....	4.5	333.447, 352.204	69.3
31675.29.....	8.5	375.979, 389.151	27.7
31878.13.....	7.5	356.072	55.8 ^c
32093.64.....	7.5	353.359, 382.915	38.1
32095.74.....	6.5	382.884	36.5
32221.57.....	7.5	381.048	33.0
32423.94.....	7.5	378.131	43.2
32464.63.....	7.5	377.550	19.3
32581.32.....	6.5	375.893	20.9
33097.72.....	8.5	356.887	75.8
36138.56.....	2.5	364.565	25.2

NOTES.—The lifetime uncertainties are all $\pm 5\%$, with one exception noted in the table. Table 1 is also available in machine-readable form in the electronic edition of the *Astrophysical Journal Supplement*.

^a Energy levels are from Blaise et al. 1984, with additional levels from <http://www.nist.gov> (2001 October).

^b Air wavelengths are computed from the energy levels using the standard index of air (Edlén 1953, 1966).

^c Uncertainty $\pm 10\%$.

3. BRANCHING FRACTIONS AND ATOMIC TRANSITION PROBABILITIES

The powerful 1 m FTS at the National Solar Observatory (NSO) was used in this work on Nd II. This instrument is uniquely suited for spectroradiometry on complex rare earth atoms and ions. It provides (1) a limit of resolution as small as 0.01 cm^{-1} , (2) wavenumber accuracy to 1 part in 10^8 , (3) broad spectral coverage from the UV to IR, and (4) the capability of recording a million point spectrum in 10 minutes. This instrument is insensitive to any small drift in source intensity, since an interferogram is a simultaneous measurement of all spectral lines. The combination of branching fractions from FTS spectra with radiative lifetimes from LIF measurements has resulted in greatly

improved atomic transition probabilities for the first and second spectra of many elements.

The emission sources for most of our Nd spectra were commercially manufactured, sealed hollow cathode discharge (HCD) lamps with fused silica windows containing either argon or neon fills. Typically, these lamps were operated at currents significantly above the manufacturers recommendation, but forced-air cooling was used to prevent overheating. The NSO 1.0 m FTS fitted with the UV beam splitter was used to record spectra during our February 2000 observing run. Spectra of the Ar-filled lamp operating at 26 mA (52 co-adds), 21.5 mA (4 co-adds), 18.5 mA (4 co-adds), and 26 mA (68 co-adds), were taken with the “super blue” silicon diode detectors and no additional filtering. The term “co-add” refers to coherently added interferogram. These spectra cover the $8000\text{--}35,000 \text{ cm}^{-1}$ region with a limit of resolution of 0.053 cm^{-1} . Spectra of the Ne-filled lamp operating at 21.5 mA (4 co-adds) and at 17 mA (4 co-adds) were taken using an identical setup. An additional spectrum of the Ar-Nd lamp at 26 mA (50 co-adds) was taken with the same setup during our February 2002 observing run. Branching fraction measurements were made almost entirely on the Ar-Nd spectra; the Ne-Nd spectra were used only to separate Ar+Nd line blends.

A search of the NSO electronic archives revealed the existence of two very useful spectra recorded on custom-built, water-cooled Ar-Nd hollow cathode discharges in 1983 July. One of these spectra has Fe lines in addition to Nd and Ar lines. Both spectra have 8 co-adds, a limit of resolution of 0.039 cm^{-1} , and extend from 6500 to $34,000 \text{ cm}^{-1}$. The UV beam splitter, “large” diode detectors, and a WG-5 filter tipped at 10° were used. John Conway was listed as the guest observer who recorded these spectra. We acknowledge his contribution.

The HCD lamps used in this study operate with relatively low buffer gas pressures and thus are not in local thermodynamic equilibrium (LTE). This is not a problem because the absolute scale of a transition probability is provided by the radiative lifetime of the upper level in every case. Doppler broadening tends to dominate the emission line shapes in these low-pressure lamps. Such narrow line shapes can produce radiation trapping or self-absorption in the lamps. By comparing spectra from the Ar-Nd lamp operating at different currents, we verified that radiation trapping is not a problem. The sputtering rate of Nd in the hollow cathode discharge, and the total Nd density in the plasma, are a strongly increasing function of discharge current.

The establishment of an accurate relative radiometric calibration or efficiency is critical to a branching fraction experiment. Detectors, spectrometer optics, lamp windows, and any other components in the light path or any reflections that contribute to the detected signal (such as due to light reflecting off the back of the hollow cathode), all have wavelength-dependent optical properties that must be taken into account when determining the ratio of line intensities at different wavelengths. Fortunately, the radiometric efficiency of the FTS is a smoothly varying function of wavelength. An excellent way to determine the relative radiometric efficiency of an FTS is to compare well-known branching ratios for sets of lines widely separated in wavelength to the intensities measured for the same lines. Sets of Ar I and Ar II lines have been established for this purpose in the range of $4300\text{--}35,000 \text{ cm}^{-1}$ by Whaling, Carle, & Pitt (1993), Hashiguchi & Hasikuni (1985), Danzmann & Kock

TABLE 2
COMPARISON OF LIFETIME MEASUREMENTS FOR ODD-PARITY LEVELS IN Nd II INCLUDING OTHER LASER-INDUCED FLUORESCENCE (LIF) AND NON-LIF MEASUREMENTS

ENERGY (cm ⁻¹)	<i>J</i>	LIFETIME (ns)				
		This Experiment LIF	Other LIF	Reference	Other Non-LIF	Reference
23229.98.....	4.5	12.5 ± 0.6	14.0 ± 0.8	1	13 ± 2	2
					13 ± 3	3
23537.38.....	4.5	25.6 ± 1.3	25.5 ± 0.8	1		
			27.7 ± 0.9	4		
23857.26.....	5.5	68.4 ± 3.4	73 ± 6	1		
24134.08.....	5.5	23.4 ± 1.2	24.9 ± 1.6	1		
24445.38.....	5.5	15.1 ± 0.8	15.5 ± 0.8	1		
24842.87.....	5.5	30.3 ± 1.5	29.7 ± 0.9	1		
25044.64.....	3.5	19.9 ± 1.0	19.5 ± 0.9	1	14 ± 3	2
25389.21.....	4.5	36.2 ± 1.8	36.3 ± 1.2	1		
25524.47.....	6.5	8.4 ± 0.4	8.7 ± 0.8	1	12 ± 1	2
25771.52.....	4.5	39.2 ± 2.0	43 ± 5	1		
25876.54.....	2.5	11.9 ± 0.6	12.4 ± 0.6	1		
25877.16.....	4.5	14.1 ± 0.7	13.6 ± 0.6	1	13 ± 2	2
					10 ± 3	3
26041.20.....	2.5	20.8 ± 1.0	21.0 ± 1.0	1		
26210.74.....	6.5	18.2 ± 0.9	18.3 ± 0.5	1		
26772.08.....	5.5	11.2 ± 0.6	11.5 ± 0.6	1	17 ± 2	2
26912.77.....	7.5	7.1 ± 0.4	7.5 ± 0.5	1	13 ± 2	2
27308.95.....	6.5	30.6 ± 1.5	24 ± 6	1		
27445.85.....	7.5	32.9 ± 1.6	15.9 ± 0.5	1		
27448.71.....	6.5	15.6 ± 0.8	15.6 ± 0.9	1		
27744.19.....	6.5	20.4 ± 1.0	20.8 ± 0.7	1	10 ± 1	2
28418.97.....	8.5	6.9 ± 0.3	7.4 ± 0.4	1	12 ± 2	2
					12 ± 3	3
28856.89.....	7.5	12.9 ± 0.6	12.7 ± 0.8	1	20 ± 5	2
29027.54.....	8.5	11.4 ± 0.6	11.9 ± 0.8	1		
30002.31.....	9.5	5.4 ± 0.3	5.7 ± 0.7	1	10 ± 1.5	2
					13 ± 3	3
30246.77.....	8.5	12.1 ± 0.6			19 ± 2	2

REFERENCES.—(1) Ward et al. 1985; (2) Gorshkov et al. 1982; (3) Andersen et al. 1975; (4) Wei et al. 1991.

(1982), and by Adams & Whaling (1981). These provide an excellent means of calibrating our FTS spectra, since the argon lines are measured in the exact experimental arrangement and at the exact same time as are the Nd II lines. A spectrum of a tungsten strip lamp, recorded immediately after the 1983 Ar-Nd spectra, was used to interpolate between Ar reference lines to improve the relative radiometric calibration of the 1983 data. A similar procedure with a tungsten-quartz-halogen lamp was used to improve the relative radiometric calibration of the more recent data. The use of a tungsten lamp is of some value near the dip in the FTS sensitivity at 12,500 cm⁻¹ from the aluminum mirror coatings, and between 10,000 and 9000 cm⁻¹, where the Si detector response is rapidly decreasing.

All possible transition wavenumbers between known energy levels of Nd II satisfying both the parity change and $\Delta J \leq 1$ selection rules were computed and used during analysis of FTS data. Energy levels from Blaise et al. (1984), supplemented with levels from Martin et al. (1978), were used to determine possible transition wavenumbers. Levels from Martin et al. (1978) are available in electronic form from the NIST database.¹

¹ Available at http://physics.nist.gov/cgi-bin/AtData/main_asd (W. C. Martin, J. Sugar, & A. Musgrove, 2000).

Branching fraction measurements were attempted on all 168 levels from the lifetime experiment, and were completed on 144 levels. The 24 levels for which branching fractions could not be completed had at least one strong branch beyond the UV limit of our spectra, or had a strong branch that was severely blended. Typically an upper level, depending on its *J* value, has about 30–35 possible transitions to known lower levels. More than 35,000 possible spectral line observations were studied during the analysis of seven different Ar-Nd spectra. Baselines and integration limits were set “interactively” during analysis of the FTS spectra. A simple numerical integration routine was used to determine the uncalibrated intensities of Nd II lines and selected Ar II and Ar I lines used to establish a relative radiometric calibration of the spectra.

The procedure for determining branching fraction uncertainties was described in detail by Wickliffe, Lawler, & Nave (2000). Branching fractions from a given upper level are defined to sum to unity; thus, a dominant line from an upper level has small branching fraction uncertainty almost by definition. Branching fractions for weaker lines near the dominant line(s) tend to have uncertainties limited by their S/N. Systematic uncertainties in the radiometric calibration are typically the most serious source of uncertainty for widely separated lines from a common upper level. A for-

mula for estimating this systematic uncertainty, presented and tested extensively by Wickliffe et al. (2000), was used here.

Branching fractions from the FTS spectra are combined with the radiative lifetime measurements described in § 2 to determine absolute transition probabilities for more than 700 lines of Nd II in Table 3. Transition probabilities for the weakest lines that were observed with poor S/N are not included in Table 3; however, these lines are included in the branching fraction normalization. Weaker lines are also more susceptible to blending problems. The effect of weaker lines becomes apparent if one sums all transition probabilities in Table 3 from a chosen upper level, and compares the sum to the inverse of the upper level lifetime from Table 1. Typically, the sum of the Table 3 transition probabilities is 85%–95% of the inverse lifetime. Although there is significant fractional uncertainty in the branching fractions for these weaker lines, this does not have much effect on the uncertainty of the stronger lines that were kept in Table 3. Branching fraction uncertainties are combined in quadrature with lifetime uncertainties to determine the transition probability uncertainties in Table 3.

Although there have been a significant number of publications on Nd II transition probabilities, there are far fewer that report original laboratory intensity measurements. Relative intensity measurements by Meggers, Corliss, & Scribner (1961) were converted to absolute transition probabilities by Corliss & Bozman (1962). Maier & Whaling (1977) reported a smaller, but high-quality set of Nd II branching fraction measurements. Ward (1985) reported a formula for renormalizing the Corliss & Bozman (1962) transition probabilities. Cowley & Corliss (1983) reported a formula for determining transition probabilities from line intensities published by Meggers, Corliss, & Scribner (1975), which are an updated version of the original Meggers et al. (1961) line intensities used by Corliss & Bozman (1962). Ward et al. (1985) determined a small set of transition probabilities based on branching fractions from Corliss & Bozman (1962) and from Maier & Whaling (1977), combined with their new lifetime measurements. Komarovski (1991) also determined a small set of transition probabilities based on branching fractions from Maier & Whaling (1977) combined with new lifetime measurements. We have limited our intensity comparisons in Table 4 to the original branching fraction measurements by Maier & Whaling. The intensity, wavelength, and temperature errors in the Corliss & Bozman data are well documented, and additional scatter plots are of limited value. Maier & Whaling devoted substantial effort to understanding and controlling systematic errors in their Nd II branching fraction measurements. Their absolute transition probabilities are not as accurate as their branching fractions, simply because they did not have access to an accurate and large set of radiative lifetimes. As is always the case, the agreement in Table 4 is best for the dominant branches, and is not quite as good for weaker branches. Uncertainty migrates to the weakest branches because branching fractions are defined so that they sum to unity. Overall, the agreement is quite good except for lines from one upper level. The most serious discordance on a strong branch is for the transition at 26271.44 cm⁻¹ from the upper level at 28856.89 cm⁻¹. The grating spectrometer used by Maier & Whaling had inadequate resolution ($\Delta\sigma = 0.54$ cm⁻¹) to separate this line from the transition at 26271.17 cm⁻¹ from the upper level at

27921.18 cm⁻¹. This blend also caused some error in other branching fractions from the same upper level as reported by Maier & Whaling. The lines are cleanly resolved in our FTS data. Problems like this are what motivated Whaling to pioneer the use of the Kitt Peak 1.0 m FTS for branching fraction measurements, and to establish radiometric calibration techniques that we still use today.

4. SOLAR AND STELLAR NEODYMIUM ABUNDANCES

The renewed attention to rare earth transition data has happily coincided with the discovery of several stars of the Galactic halo that have very low metallicities ([Fe/H] < -2)² but extremely large relative overabundances of *n*-capture elements ([*n*-capture/Fe] > +1). Such *n*-capture-rich stars present unique absorption spectra, which in extreme cases exhibit *n*-capture transitions that rival the strengths of Fe-peak lines. In this section we apply the new Nd II transition probability data first to the solar spectrum and then to three *n*-capture-rich stars that have been studied previously by our group.

4.1. The Solar Photospheric Nd Abundance

Compendiums and reviews of solar system abundances (e.g., Anders & Grevesse 1989; Grevesse & Noels 1993; Grevesse, Noels, & Sauval 1996; Grevesse & Sauval 1998, 2002; Lodders 2003) suggest that among the rare earth elements, Nd, Tb, Ho, Tm, Yb, and Lu have large photospheric abundance uncertainties (≥ 0.10 dex). For most of these elements the dominant abundance error sources are intrinsic to the solar spectrum. That is, their only detectable spectral features are few in number, and/or are extremely weak, and/or occur in relatively inaccessible spectral regions, and/or are extremely blended. For example, Moore, Minnaert, & Houtgast (1966) identify only five Tb II lines in the solar spectrum, and Lawler et al. (2001b) were able to employ only three of these in their photospheric abundance analysis. In contrast, Nd exhibits a rich solar spectrum. Moore et al. list 102 solar Nd II lines. With so many features to choose from, the Nd abundance accuracy has been limited by transition probability uncertainties. Solar abundance reviews have adopted the value derived by Ward et al. (1985), $\log \epsilon(\text{Nd}) = 1.50 \pm 0.12$. This abundance has not been updated in the last two decades.

Our new Nd II analysis generally follows the procedures employed previously for La II (Lawler et al. 2001a), Tb II (Lawler et al. 2001b), and Eu II (Lawler et al. 2001c). However, unlike those other species, there are nearly 100 detectable Nd II lines potentially available for an abundance analysis. Therefore, we were able to concentrate on just the best (i.e., the strongest, least blended) transitions and still have a large solar Nd line list. We began by identifying detectable Nd II features in the solar center-of-disk spectrum of Delbouille, Neven, & Roland (1973), immediately eliminating the most blended ones. Further culling was accomplished with the help of the solar spectral atlas of

² We adopt standard stellar spectroscopic notation in this section. Abundances relative to the Sun are defined as $[A/B] \equiv \log_{10}(N_A/N_B)_{\text{star}} - \log_{10}(N_A/N_B)_{\odot}$, and “absolute” abundances as $\log \epsilon(A) \equiv \log_{10}(N_A/N_H) + 12.0$, for elements A and B. Metallicity is assumed to be equivalent to the stellar [Fe/H] value.

TABLE 3
ATOMIC TRANSITION PROBABILITIES FOR Nd II ARRANGED BY WAVENUMBER

Transition Wavenumber (cm ⁻¹)	λ in Air (nm)	Upper Level (cm ⁻¹)	Upper J	Lower Level (cm ⁻¹)	Lower J	Transition Probability (10 ⁶ s ⁻¹)	$\log_{10} gf$	Notes ^a
31186.58.....	320.558	31186.58	3.5	0.00	3.5	0.90 ± 0.09	-1.95	
30937.97.....	323.134	31451.30	4.5	513.33	4.5	0.75 ± 0.08	-1.93	
30673.25.....	325.923	31186.58	3.5	513.33	4.5	5.2 ± 0.4	-1.18	
30666.43.....	325.996	31179.76	4.5	513.33	4.5	0.59 ± 0.05	-2.03	
30037.08.....	332.826	30037.08	2.5	0.00	3.5	18.5 ± 1.0	-0.73	
29981.19.....	333.447	31451.30	4.5	1470.10	5.5	7.0 ± 0.4	-0.93	
29940.01.....	333.905	30453.34	3.5	513.33	4.5	8.6 ± 0.5	-0.94	
29879.17.....	334.585	32464.63	7.5	2585.46	6.5	0.32 ± 0.06	-2.06	
29801.09.....	335.462	31451.30	4.5	1650.20	4.5	1.79 ± 0.16	-1.52	
29709.65.....	336.494	31179.76	4.5	1470.10	5.5	7.5 ± 0.4	-0.90	
29683.75.....	336.788	31153.86	6.5	1470.10	5.5	0.27 ± 0.04	-2.19	a
29636.11.....	337.329	32221.57	7.5	2585.46	6.5	0.61 ± 0.06	-1.78	
29529.55.....	338.547	31179.76	4.5	1650.20	4.5	0.39 ± 0.04	-2.17	
29343.00.....	340.699	30813.11	6.5	1470.10	5.5	0.63 ± 0.06	-1.82	
29292.67.....	341.284	31878.13	7.5	2585.46	6.5	0.50 ± 0.08	-1.86	
29230.67.....	342.008	30700.78	6.5	1470.10	5.5	0.59 ± 0.06	-1.84	
29100.11.....	343.543	30570.21	6.5	1470.10	5.5	0.78 ± 0.06	-1.71	
28926.24.....	345.608	28926.24	4.5	0.00	3.5	0.150 ± 0.022	-2.57	
28878.23.....	346.182	30348.34	6.5	1470.10	5.5	0.66 ± 0.05	-1.78	
28823.40.....	346.841	29336.73	5.5	513.33	4.5	1.87 ± 0.14	-1.39	
28803.14.....	347.085	30453.34	3.5	1650.20	4.5	4.20 ± 0.25	-1.22	
28785.29.....	347.300	29298.63	4.5	513.33	4.5	0.32 ± 0.04	-2.24	
28662.70.....	348.786	32464.63	7.5	3801.93	7.5	0.82 ± 0.08	-1.62	
28523.32.....	350.490	29036.65	3.5	513.33	4.5	0.144 ± 0.019	-2.67	
28419.64.....	351.769	32221.57	7.5	3801.93	7.5	0.62 ± 0.07	-1.74	
28412.91.....	351.852	28926.24	4.5	513.33	4.5	0.33 ± 0.03	-2.21	
28384.54.....	352.204	31451.30	4.5	3066.75	5.5	2.84 ± 0.19	-1.28	
28340.55.....	352.750	28340.55	4.5	0.00	3.5	0.80 ± 0.07	-1.83	
28298.46.....	353.275	28298.46	4.5	0.00	3.5	0.70 ± 0.06	-1.88	
28291.71.....	353.359	32093.64	7.5	3801.93	7.5	3.72 ± 0.23	-0.95	
28231.37.....	354.115	29701.47	6.5	1470.10	5.5	0.42 ± 0.05	-1.95	
28227.65.....	354.161	30813.11	6.5	2585.46	6.5	1.89 ± 0.14	-1.30	
28213.87.....	354.334	28213.87	3.5	0.00	3.5	5.6 ± 0.4	-1.07	
28190.01.....	354.634	31256.77	6.5	3066.75	5.5	0.58 ± 0.09	-1.82	
28170.45.....	354.881	28170.45	4.5	0.00	3.5	0.45 ± 0.04	-2.08	
28115.32.....	355.576	30700.78	6.5	2585.46	6.5	4.24 ± 0.23	-0.95	
28087.10.....	355.934	31153.86	6.5	3066.75	5.5	0.66 ± 0.07	-1.75	
28076.20.....	356.072	31878.13	7.5	3801.93	7.5	10.5 ± 1.1	-0.50	
28012.08.....	356.887	33097.72	8.5	5085.64	8.5	11.3 ± 0.6	-0.41	
27984.75.....	357.235	30570.21	6.5	2585.46	6.5	0.65 ± 0.08	-1.76	
27964.15.....	357.499	29434.26	6.5	1470.10	5.5	0.67 ± 0.06	-1.74	
27934.52.....	357.878	27934.52	4.5	0.00	3.5	0.92 ± 0.07	-1.75	
27921.38.....	358.046	27921.38	4.5	0.00	3.5	0.65 ± 0.08	-1.90	
27866.63.....	358.750	29336.73	5.5	1470.10	5.5	9.6 ± 0.5	-0.65	
27834.40.....	359.165	29484.61	5.5	1650.20	4.5	0.64 ± 0.06	-1.82	
27827.22.....	359.258	28340.55	4.5	513.33	4.5	6.5 ± 0.4	-0.90	
27805.38.....	359.540	27805.38	3.5	0.00	3.5	2.03 ± 0.12	-1.50	
27785.13.....	359.802	28298.46	4.5	513.33	4.5	4.91 ± 0.27	-1.02	
27762.88.....	360.090	30348.34	6.5	2585.46	6.5	5.01 ± 0.27	-0.86	
27720.69.....	360.638	30306.15	7.5	2585.46	6.5	0.63 ± 0.06	-1.71	
27709.08.....	360.790	32221.57	7.5	4512.50	6.5	1.08 ± 0.10	-1.47	
27700.54.....	360.901	28213.87	3.5	513.33	4.5	0.28 ± 0.04	-2.36	
27694.62.....	360.978	27694.62	3.5	0.00	3.5	10.2 ± 0.5	-0.80	
27686.53.....	361.084	29336.73	5.5	1650.20	4.5	0.56 ± 0.06	-1.88	
27657.12.....	361.468	28170.45	4.5	513.33	4.5	1.75 ± 0.15	-1.46	
27648.42.....	361.581	29298.63	4.5	1650.20	4.5	8.9 ± 0.5	-0.76	
27634.02.....	361.770	30700.78	6.5	3066.75	5.5	0.39 ± 0.04	-1.97	
27618.62.....	361.971	29088.72	6.5	1470.10	5.5	0.51 ± 0.04	-1.85	
27589.18.....	362.358	29239.38	5.5	1650.20	4.5	0.31 ± 0.03	-2.14	
27581.15.....	362.463	32093.64	7.5	4512.50	6.5	4.25 ± 0.29	-0.87	
27560.19.....	362.739	31362.12	7.5	3801.93	7.5	0.89 ± 0.08	-1.55	
27509.39.....	363.409	30094.85	7.5	2585.46	6.5	0.41 ± 0.04	-1.89	
27504.11.....	363.478	27504.11	3.5	0.00	3.5	0.67 ± 0.05	-1.97	

TABLE 3—Continued

Transition Wavenumber (cm ⁻¹)	λ in Air (nm)	Upper Level (cm ⁻¹)	Upper J	Lower Level (cm ⁻¹)	Lower J	Transition Probability (10 ⁶ s ⁻¹)	$\log_{10} gf$	Notes ^a
27503.46.....	363.487	30570.21	6.5	3066.75	5.5	4.1 ± 0.3	-0.94	
27479.10.....	363.809	27992.43	5.5	513.33	4.5	0.42 ± 0.04	-2.00	
27456.14.....	364.113	28926.24	4.5	1470.10	5.5	0.20 ± 0.03	-2.40	
27454.84.....	364.131	31256.77	6.5	3801.93	7.5	0.37 ± 0.06	-1.99	
27444.53.....	364.268	27444.53	3.5	0.00	3.5	0.383 ± 0.029	-2.21	
27421.19.....	364.578	27934.52	4.5	513.33	4.5	3.55 ± 0.21	-1.15	
27408.05.....	364.752	27921.38	4.5	513.33	4.5	0.47 ± 0.05	-2.02	
27390.06.....	364.992	28860.16	5.5	1470.10	5.5	0.65 ± 0.07	-1.81	
27386.45.....	365.040	29036.65	3.5	1650.20	4.5	4.65 ± 0.25	-1.13	
27365.64.....	365.318	31878.13	7.5	4512.50	6.5	2.73 ± 0.30	-1.06	
27351.93.....	365.501	31153.86	6.5	3801.93	7.5	2.94 ± 0.19	-1.08	
27292.05.....	366.303	27805.38	3.5	513.33	4.5	1.16 ± 0.08	-1.73	
27281.58.....	366.443	30348.34	6.5	3066.75	5.5	0.54 ± 0.05	-1.81	
27276.04.....	366.518	28926.24	4.5	1650.20	4.5	10.8 ± 0.6	-0.66	
27255.83.....	366.790	28725.93	6.5	1470.10	5.5	0.41 ± 0.04	-1.93	
27233.53.....	367.090	27233.53	4.5	0.00	3.5	1.24 ± 0.12	-1.60	
27209.96.....	367.408	28860.16	5.5	1650.20	4.5	0.82 ± 0.06	-1.70	
27181.29.....	367.795	27694.62	3.5	513.33	4.5	0.53 ± 0.05	-2.07	
27179.60.....	367.818	27179.60	4.5	0.00	3.5	2.00 ± 0.13	-1.39	
27135.93.....	368.410	32221.57	7.5	5085.64	8.5	1.45 ± 0.11	-1.33	
27116.01.....	368.681	29701.47	6.5	2585.46	6.5	0.35 ± 0.04	-2.01	
27093.38.....	368.989	28563.48	6.5	1470.10	5.5	0.28 ± 0.03	-2.09	
27014.27.....	370.069	27014.27	4.5	0.00	3.5	0.76 ± 0.06	-1.81	
27008.00.....	370.155	32093.64	7.5	5085.64	8.5	1.16 ± 0.11	-1.42	
26926.99.....	371.269	26926.99	4.5	0.00	3.5	0.68 ± 0.06	-1.85	
26898.85.....	371.657	30700.78	6.5	3801.93	7.5	2.14 ± 0.13	-1.21	
26884.30.....	371.859	28354.40	6.5	1470.10	5.5	1.71 ± 0.10	-1.30	
26870.44.....	372.050	28340.55	4.5	1470.10	5.5	1.85 ± 0.19	-1.42	
26849.62.....	372.339	31362.12	7.5	4512.50	6.5	0.34 ± 0.04	-1.95	
26848.80.....	372.350	29434.26	6.5	2585.46	6.5	13.7 ± 0.8	-0.40	
26838.96.....	372.487	27352.29	5.5	513.33	4.5	4.80 ± 0.26	-0.92	
26828.36.....	372.634	28298.46	4.5	1470.10	5.5	1.37 ± 0.09	-1.54	
26815.50.....	372.813	28285.61	5.5	1470.10	5.5	12.6 ± 0.7	-0.50	
26793.33.....	373.121	26793.33	3.5	0.00	3.5	3.0 ± 0.3	-1.30	
26792.49.....	373.133	31878.13	7.5	5085.64	8.5	1.80 ± 0.20	-1.22	
26768.28.....	373.470	30570.21	6.5	3801.93	7.5	2.41 ± 0.14	-1.15	
26751.27.....	373.708	29336.73	5.5	2585.46	6.5	7.8 ± 0.4	-0.71	
26744.27.....	373.806	31256.77	6.5	4512.50	6.5	30.8 ± 1.6	-0.04	
26720.20.....	374.142	27233.53	4.5	513.33	4.5	9.9 ± 0.5	-0.68	
26666.27.....	374.899	27179.60	4.5	513.33	4.5	1.16 ± 0.07	-1.61	
26653.92.....	375.073	29239.38	5.5	2585.46	6.5	2.31 ± 0.13	-1.23	
26641.36.....	375.250	31153.86	6.5	4512.50	6.5	24.3 ± 1.3	-0.14	
26640.08.....	375.268	26640.08	3.5	0.00	3.5	8.9 ± 0.5	-0.82	
26635.40.....	375.333	28285.61	5.5	1650.20	4.5	1.01 ± 0.07	-1.59	
26619.37.....	375.560	28089.47	6.5	1470.10	5.5	4.88 ± 0.27	-0.84	
26603.65.....	375.781	30405.58	7.5	3801.93	7.5	9.1 ± 0.5	-0.51	
26595.74.....	375.893	32581.32	6.5	5985.58	7.5	39.4 ± 2.1	0.07	
26589.65.....	375.979	31675.29	8.5	5085.64	8.5	9.3 ± 0.5	-0.45	
26563.66.....	376.347	28213.87	3.5	1650.20	4.5	21.8 ± 1.1	-0.43	
26546.41.....	376.592	30348.34	6.5	3801.93	7.5	2.23 ± 0.14	-1.18	
26522.32.....	376.934	27992.43	5.5	1470.10	5.5	1.36 ± 0.09	-1.46	
26520.24.....	376.963	28170.45	4.5	1650.20	4.5	8.5 ± 0.5	-0.74	
26519.93.....	376.968	27990.04	4.5	1470.10	5.5	1.83 ± 0.12	-1.41	
26503.26.....	377.205	29088.72	6.5	2585.46	6.5	3.28 ± 0.19	-1.01	
26500.94.....	377.238	27014.27	4.5	513.33	4.5	2.02 ± 0.12	-1.37	
26479.05.....	377.550	32464.63	7.5	5985.58	7.5	38.9 ± 2.1	0.12	
26478.56.....	377.557	26991.89	5.5	513.33	4.5	1.09 ± 0.09	-1.55	
26464.41.....	377.759	27934.52	4.5	1470.10	5.5	0.54 ± 0.07	-1.93	
26451.28.....	377.946	27921.38	4.5	1470.10	5.5	12.8 ± 0.8	-0.56	
26444.84.....	378.038	30246.77	8.5	3801.93	7.5	11.6 ± 0.6	-0.35	
26422.54.....	378.357	26422.54	3.5	0.00	3.5	1.19 ± 0.07	-1.69	
26417.85.....	378.424	29484.61	5.5	3066.75	5.5	55.4 ± 2.8	0.15	
26413.66.....	378.484	26926.99	4.5	513.33	4.5	4.29 ± 0.24	-1.04	
26367.50.....	379.147	29434.26	6.5	3066.75	5.5	0.80 ± 0.06	-1.62	
26342.22.....	379.511	27992.43	5.5	1650.20	4.5	0.325 ± 0.026	-2.07	

TABLE 3—Continued

Transition Wavenumber (cm ⁻¹)	λ in Air (nm)	Upper Level (cm ⁻¹)	Upper <i>J</i>	Lower Level (cm ⁻¹)	Lower <i>J</i>	Transition Probability (10 ⁶ s ⁻¹)	$\log_{10} gf$	Notes ^a
26339.83.....	379.545	27990.04	4.5	1650.20	4.5	10.4 ± 0.5	-0.65	
26313.61.....	379.924	28899.07	6.5	2585.46	6.5	2.60 ± 0.14	-1.10	
26300.61.....	380.111	30813.11	6.5	4512.50	6.5	8.8 ± 0.5	-0.57	
26299.33.....	380.130	27769.43	5.5	1470.10	5.5	2.01 ± 0.12	-1.28	
26292.92.....	380.223	30094.85	7.5	3801.93	7.5	2.72 ± 0.17	-1.03	
26284.31.....	380.347	27934.52	4.5	1650.20	4.5	18.8 ± 1.0	-0.39	
26280.00.....	380.410	26793.33	3.5	513.33	4.5	1.83 ± 0.19	-1.50	
26276.48.....	380.461	31362.12	7.5	5085.64	8.5	0.53 ± 0.06	-1.73	
26274.70.....	380.486	28860.16	5.5	2585.46	6.5	3.28 ± 0.18	-1.07	
26274.08.....	380.495	27744.19	6.5	1470.10	5.5	0.130 ± 0.020	-2.40	
26271.43.....	380.534	28856.89	7.5	2585.46	6.5	15.5 ± 0.9	-0.27	
26271.18.....	380.537	27921.38	4.5	1650.20	4.5	40.5 ± 2.1	-0.06	
26269.98.....	380.555	29336.73	5.5	3066.75	5.5	10.1 ± 0.5	-0.58	
26258.75.....	380.717	26772.08	5.5	513.33	4.5	1.19 ± 0.09	-1.51	
26251.32.....	380.825	27721.43	6.5	1470.10	5.5	2.71 ± 0.15	-1.08	
26247.77.....	380.877	26761.10	5.5	513.33	4.5	8.6 ± 0.5	-0.65	
26245.89.....	380.904	26759.22	4.5	513.33	4.5	7.8 ± 0.4	-0.77	
26235.99.....	381.048	32221.57	7.5	5985.58	7.5	21.0 ± 1.1	-0.14	
26231.87.....	381.107	29298.63	4.5	3066.75	5.5	6.6 ± 0.4	-0.84	
26227.09.....	381.177	26227.09	4.5	0.00	3.5	2.53 ± 0.15	-1.26	
26206.80.....	381.472	26206.80	3.5	0.00	3.5	14.4 ± 0.8	-0.60	
26172.63.....	381.970	29239.38	5.5	3066.75	5.5	6.0 ± 0.3	-0.80	
26155.18.....	382.225	27805.38	3.5	1650.20	4.5	1.80 ± 0.11	-1.50	
26144.28.....	382.384	28729.74	7.5	2585.46	6.5	0.38 ± 0.03	-1.87	
26140.47.....	382.440	28725.93	6.5	2585.46	6.5	0.98 ± 0.08	-1.52	
26126.75.....	382.641	26640.08	3.5	513.33	4.5	22.1 ± 1.1	-0.41	
26119.23.....	382.751	27769.43	5.5	1650.20	4.5	1.69 ± 0.09	-1.35	
26116.03.....	382.798	26116.03	2.5	0.00	3.5	8.6 ± 0.5	-0.94	
26108.06.....	382.915	32093.64	7.5	5985.58	7.5	11.0 ± 0.6	-0.41	
26083.40.....	383.277	27553.50	4.5	1470.10	5.5	2.89 ± 0.17	-1.20	
26057.72.....	383.655	30570.21	6.5	4512.50	6.5	14.0 ± 0.8	-0.36	
26048.30.....	383.793	27518.40	5.5	1470.10	5.5	5.05 ± 0.26	-0.87	
26044.41.....	383.851	27694.62	3.5	1650.20	4.5	1.74 ± 0.11	-1.51	
26041.20.....	383.898	26041.20	2.5	0.00	3.5	43.3 ± 2.2	-0.24	
25987.07.....	384.698	26500.40	4.5	513.33	4.5	1.17 ± 0.07	-1.59	
25978.61.....	384.823	27448.71	6.5	1470.10	5.5	17.9 ± 1.0	-0.25	
25978.02.....	384.832	28563.48	6.5	2585.46	6.5	16.1 ± 0.8	-0.30	
25955.49.....	385.166	28540.95	7.5	2585.46	6.5	9.1 ± 0.5	-0.49	
25909.21.....	385.854	26422.54	3.5	513.33	4.5	4.23 ± 0.24	-1.12	
25903.30.....	385.942	27553.50	4.5	1650.20	4.5	3.87 ± 0.21	-1.06	
25899.54.....	385.998	29701.47	6.5	3801.93	7.5	0.38 ± 0.04	-1.92	
25893.08.....	386.094	30405.58	7.5	4512.50	6.5	8.0 ± 0.4	-0.54	
25892.55.....	386.102	31878.13	7.5	5985.58	7.5	0.62 ± 0.09	-1.66	
25882.18.....	386.257	27352.29	5.5	1470.10	5.5	6.5 ± 0.3	-0.76	
25877.16.....	386.332	25877.16	4.5	0.00	3.5	11.7 ± 0.7	-0.58	
25876.54.....	386.341	25876.54	2.5	0.00	3.5	72 ± 4	-0.01	
25868.20.....	386.465	27518.40	5.5	1650.20	4.5	2.75 ± 0.15	-1.13	
25867.40.....	386.477	26380.73	4.5	513.33	4.5	0.99 ± 0.06	-1.66	
25853.91.....	386.679	27504.11	3.5	1650.20	4.5	6.2 ± 0.3	-0.95	
25838.84.....	386.905	27308.95	6.5	1470.10	5.5	11.6 ± 0.6	-0.44	
25832.32.....	387.002	28899.07	6.5	3066.75	5.5	0.68 ± 0.04	-1.67	
25794.32.....	387.572	27444.53	3.5	1650.20	4.5	7.5 ± 0.4	-0.87	
25793.41.....	387.586	28860.16	5.5	3066.75	5.5	14.1 ± 0.7	-0.42	
25775.34.....	387.858	27245.45	5.5	1470.10	5.5	13.6 ± 1.1	-0.43	
25771.52.....	387.915	25771.52	4.5	0.00	3.5	0.96 ± 0.06	-1.67	
25768.94.....	387.954	28354.40	6.5	2585.46	6.5	19.5 ± 1.0	-0.21	
25763.42.....	388.037	27233.53	4.5	1470.10	5.5	11.4 ± 0.6	-0.59	
25760.76.....	388.077	26274.09	5.5	513.33	4.5	17.9 ± 0.9	-0.31	
25713.76.....	388.787	26227.09	4.5	513.33	4.5	7.4 ± 0.4	-0.78	
25702.08.....	388.963	27352.29	5.5	1650.20	4.5	1.84 ± 0.10	-1.30	
25700.15.....	388.993	28285.61	5.5	2585.46	6.5	28.9 ± 1.5	-0.10	
25695.85.....	389.058	30781.49	8.5	5085.64	8.5	38.0 ± 2.0	0.19	
25693.47.....	389.094	26206.80	3.5	513.33	4.5	33.4 ± 1.7	-0.22	
25689.71.....	389.151	31675.29	8.5	5985.58	7.5	17.8 ± 0.9	-0.14	
25669.15.....	389.462	26182.48	5.5	513.33	4.5	10.1 ± 0.5	-0.56	

TABLE 3—Continued

Transition Wavenumber (cm ⁻¹)	λ in Air (nm)	Upper Level (cm ⁻¹)	Upper <i>J</i>	Lower Level (cm ⁻¹)	Lower <i>J</i>	Transition Probability (10 ⁶ s ⁻¹)	$\log_{10} gf$	Notes ^a
25659.18.....	389.614	28725.93	6.5	3066.75	5.5	4.48 ± 0.25	-0.85	
25632.33.....	390.022	29434.26	6.5	3801.93	7.5	39.5 ± 2.0	0.10	
25610.69.....	390.351	28196.15	6.5	2585.46	6.5	1.45 ± 0.10	-1.33	
25595.24.....	390.587	27245.45	5.5	1650.20	4.5	19.0 ± 1.5	-0.28	
25582.35.....	390.784	30094.85	7.5	4512.50	6.5	15.0 ± 0.8	-0.26	
25560.59.....	391.117	29362.52	7.5	3801.93	7.5	34.7 ± 1.8	0.11	
25544.16.....	391.368	27014.27	4.5	1470.10	5.5	3.21 ± 0.18	-1.13	
25529.40.....	391.594	27179.60	4.5	1650.20	4.5	8.3 ± 0.4	-0.72	
25521.79.....	391.711	26991.89	5.5	1470.10	5.5	0.88 ± 0.06	-1.62	
25504.01.....	391.984	28089.47	6.5	2585.46	6.5	1.95 ± 0.12	-1.20	
25496.73.....	392.096	28563.48	6.5	3066.75	5.5	31.8 ± 1.6	0.01	
25458.81.....	392.680	29260.74	7.5	3801.93	7.5	0.39 ± 0.07	-1.84	
25456.89.....	392.710	26926.99	4.5	1470.10	5.5	11.2 ± 0.6	-0.59	
25406.97.....	393.481	27992.43	5.5	2585.46	6.5	13.7 ± 0.7	-0.42	
25389.21.....	393.757	25389.21	4.5	0.00	3.5	1.24 ± 0.07	-1.54	
25376.54.....	393.953	31362.12	7.5	5985.58	7.5	5.03 ± 0.27	-0.73	
25363.83.....	394.151	25877.16	4.5	513.33	4.5	41.3 ± 2.1	-0.02	
25341.69.....	394.495	26991.89	5.5	1650.20	4.5	0.180 ± 0.023	-2.30	
25319.94.....	394.834	30405.58	7.5	5085.64	8.5	7.1 ± 0.4	-0.58	
25301.98.....	395.114	26772.08	5.5	1470.10	5.5	39.3 ± 2.0	0.04	
25295.28.....	395.219	25295.28	3.5	0.00	3.5	21.5 ± 1.1	-0.39	
25290.99.....	395.286	26761.10	5.5	1470.10	5.5	7.6 ± 0.4	-0.67	
25287.65.....	395.338	28354.40	6.5	3066.75	5.5	3.30 ± 0.23	-0.97	
25286.79.....	395.351	29088.72	6.5	3801.93	7.5	12.5 ± 0.7	-0.39	
25276.79.....	395.508	26926.99	4.5	1650.20	4.5	1.86 ± 0.14	-1.36	
25273.79.....	395.555	28340.55	4.5	3066.75	5.5	0.80 ± 0.12	-1.73	
25271.19.....	395.596	31256.77	6.5	5985.58	7.5	7.6 ± 0.5	-0.60	
25268.68.....	395.635	26738.79	6.5	1470.10	5.5	0.70 ± 0.06	-1.64	
25258.19.....	395.799	25771.52	4.5	513.33	4.5	9.0 ± 0.5	-0.67	
25231.33.....	396.220	27816.79	7.5	2585.46	6.5	7.1 ± 0.4	-0.57	
25225.61.....	396.310	29027.54	8.5	3801.93	7.5	39.8 ± 2.0	0.23	
25220.51.....	396.391	30306.15	7.5	5085.64	8.5	11.4 ± 0.6	-0.37	
25218.85.....	396.417	28285.61	5.5	3066.75	5.5	2.60 ± 0.15	-1.13	
25188.98.....	396.887	29701.47	6.5	4512.50	6.5	8.8 ± 0.5	-0.54	
25183.97.....	396.966	27769.43	5.5	2585.46	6.5	2.77 ± 0.15	-1.11	
25161.13.....	397.326	30246.77	8.5	5085.64	8.5	53.6 ± 2.7	0.36	
25158.73.....	397.364	27744.19	6.5	2585.46	6.5	22.4 ± 1.2	-0.13	
25143.13.....	397.611	26793.33	3.5	1650.20	4.5	1.63 ± 0.17	-1.51	
25138.55.....	397.683	25138.55	3.5	0.00	3.5	21.0 ± 1.1	-0.40	
25135.97.....	397.724	27721.43	6.5	2585.46	6.5	1.45 ± 0.09	-1.32	
25129.40.....	397.828	28196.15	6.5	3066.75	5.5	1.31 ± 0.09	-1.36	
25121.88.....	397.947	26772.08	5.5	1650.20	4.5	16.5 ± 0.9	-0.33	
25110.89.....	398.121	26761.10	5.5	1650.20	4.5	4.36 ± 0.24	-0.91	
25109.02.....	398.151	26759.22	4.5	1650.20	4.5	0.71 ± 0.05	-1.77	
25103.69.....	398.235	28170.45	4.5	3066.75	5.5	9.4 ± 0.5	-0.65	
25097.14.....	398.339	28899.07	6.5	3801.93	7.5	3.17 ± 0.17	-0.98	
25054.96.....	399.010	28856.89	7.5	3801.93	7.5	35.7 ± 1.9	0.13	
25044.64.....	399.174	25044.64	3.5	0.00	3.5	28.9 ± 1.5	-0.26	
25030.30.....	399.403	26500.40	4.5	1470.10	5.5	1.40 ± 0.08	-1.48	
25026.26.....	399.467	27611.72	7.5	2585.46	6.5	28.6 ± 1.5	0.04	
25022.72.....	399.524	28089.47	6.5	3066.75	5.5	3.97 ± 0.23	-0.88	
25009.21.....	399.740	30094.85	7.5	5085.64	8.5	4.12 ± 0.25	-0.80	
24989.88.....	400.049	26640.08	3.5	1650.20	4.5	7.5 ± 0.4	-0.84	
24972.11.....	400.334	29484.61	5.5	4512.50	6.5	1.13 ± 0.09	-1.49	
24967.94.....	400.400	25481.27	5.5	513.33	4.5	9.3 ± 0.8	-0.57	
24946.60.....	400.743	28748.53	8.5	3801.93	7.5	9.1 ± 0.5	-0.40	
24932.94.....	400.962	27518.40	5.5	2585.46	6.5	1.02 ± 0.06	-1.53	
24927.81.....	401.045	28729.74	7.5	3801.93	7.5	2.64 ± 0.15	-0.99	
24924.00.....	401.106	28725.93	6.5	3801.93	7.5	5.19 ± 0.29	-0.76	
24923.28.....	401.118	27990.04	4.5	3066.75	5.5	0.76 ± 0.06	-1.74	
24921.76.....	401.142	29434.26	6.5	4512.50	6.5	0.49 ± 0.04	-1.78	
24916.67.....	401.224	30002.31	9.5	5085.64	8.5	134 ± 7	0.81	
24913.85.....	401.270	24913.85	3.5	0.00	3.5	13.1 ± 0.7	-0.60	
24910.62.....	401.322	26380.73	4.5	1470.10	5.5	3.31 ± 0.17	-1.10	
24875.88.....	401.882	25389.21	4.5	513.33	4.5	5.9 ± 0.3	-0.85	

TABLE 3—Continued

Transition Wavenumber (cm ⁻¹)	λ in Air (nm)	Upper Level (cm ⁻¹)	Upper J	Lower Level (cm ⁻¹)	Lower J	Transition Probability (10 ⁶ s ⁻¹)	$\log_{10} gf$	Notes ^a
24863.25.....	402.086	27448.71	6.5	2585.46	6.5	18.9 ± 1.0	-0.19	
24860.39.....	402.133	27445.85	7.5	2585.46	6.5	20.7 ± 1.1	-0.10	
24857.91.....	402.173	26328.02	6.5	1470.10	5.5	14.4 ± 0.8	-0.31	
24854.63.....	402.226	27921.38	4.5	3066.75	5.5	1.39 ± 0.19	-1.47	
24850.20.....	402.298	26500.40	4.5	1650.20	4.5	1.66 ± 0.10	-1.40	
24850.02.....	402.300	29362.52	7.5	4512.50	6.5	28.2 ± 1.5	0.04	
24839.04.....	402.478	25352.37	5.5	513.33	4.5	4.82 ± 0.26	-0.85	
24827.53.....	402.665	30813.11	6.5	5985.58	7.5	2.56 ± 0.17	-1.06	
24803.98.....	403.047	26274.09	5.5	1470.10	5.5	6.9 ± 0.4	-0.70	
24795.91.....	403.178	30781.49	8.5	5985.58	7.5	42.0 ± 2.2	0.27	
24781.95.....	403.406	25295.28	3.5	513.33	4.5	0.95 ± 0.06	-1.73	
24772.33.....	403.562	26422.54	3.5	1650.20	4.5	0.280 ± 0.025	-2.26	
24766.83.....	403.652	27352.29	5.5	2585.46	6.5	0.83 ± 0.05	-1.61	
24761.55.....	403.738	28563.48	6.5	3801.93	7.5	1.03 ± 0.09	-1.45	
24756.98.....	403.812	26227.09	4.5	1470.10	5.5	3.65 ± 0.22	-1.05	
24748.25.....	403.955	29260.74	7.5	4512.50	6.5	1.72 ± 0.11	-1.17	
24740.64.....	404.079	26210.74	6.5	1470.10	5.5	38.2 ± 2.0	0.12	
24739.02.....	404.106	28540.95	7.5	3801.93	7.5	7.6 ± 0.4	-0.53	
24730.52.....	404.244	26380.73	4.5	1650.20	4.5	1.92 ± 0.10	-1.33	
24723.49.....	404.359	27308.95	6.5	2585.46	6.5	5.7 ± 0.3	-0.71	
24712.38.....	404.541	26182.48	5.5	1470.10	5.5	0.190 ± 0.026	-2.25	
24702.68.....	404.700	27769.43	5.5	3066.75	5.5	0.71 ± 0.07	-1.68	
24677.43.....	405.114	27744.19	6.5	3066.75	5.5	14.5 ± 0.8	-0.30	
24654.67.....	405.488	27721.43	6.5	3066.75	5.5	2.33 ± 0.13	-1.09	
24625.22.....	405.973	25138.55	3.5	513.33	4.5	0.66 ± 0.05	-1.89	
24623.88.....	405.995	26274.09	5.5	1650.20	4.5	10.3 ± 0.6	-0.52	
24617.04.....	406.108	28418.97	8.5	3801.93	7.5	80 ± 4	0.55	
24576.88.....	406.772	26227.09	4.5	1650.20	4.5	0.98 ± 0.07	-1.61	
24569.77.....	406.889	24569.77	4.5	0.00	3.5	1.51 ± 0.08	-1.42	
24567.53.....	406.926	25080.86	5.5	513.33	4.5	8.9 ± 0.9	-0.57	
24561.10.....	407.033	27146.56	6.5	2585.46	6.5	0.44 ± 0.04	-1.82	
24556.60.....	407.108	26206.80	3.5	1650.20	4.5	0.327 ± 0.027	-2.19	
24552.47.....	407.176	28354.40	6.5	3801.93	7.5	2.32 ± 0.17	-1.09	
24532.28.....	407.511	26182.48	5.5	1650.20	4.5	11.0 ± 0.6	-0.48	
24531.31.....	407.527	25044.64	3.5	513.33	4.5	8.8 ± 0.5	-0.76	
24501.58.....	408.022	25014.91	5.5	513.33	4.5	3.6 ± 0.4	-0.97	
24486.75.....	408.269	27553.50	4.5	3066.75	5.5	0.88 ± 0.06	-1.66	
24468.03.....	408.581	24468.03	3.5	0.00	3.5	3.42 ± 0.18	-1.16	
24451.65.....	408.855	27518.40	5.5	3066.75	5.5	1.75 ± 0.13	-1.28	
24407.06.....	409.602	25877.16	4.5	1470.10	5.5	0.32 ± 0.04	-2.09	
24406.43.....	409.612	26991.89	5.5	2585.46	6.5	6.0 ± 0.3	-0.74	
24394.22.....	409.817	28196.15	6.5	3801.93	7.5	6.6 ± 0.3	-0.63	
24381.96.....	410.024	27448.71	6.5	3066.75	5.5	3.85 ± 0.21	-0.87	
24347.67.....	410.601	28860.16	5.5	4512.50	6.5	0.75 ± 0.09	-1.64	
24344.40.....	410.656	28856.89	7.5	4512.50	6.5	2.20 ± 0.13	-1.05	
24329.54.....	410.907	24842.87	5.5	513.33	4.5	22.6 ± 1.2	-0.16	
24327.31.....	410.945	26912.77	7.5	2585.46	6.5	55.2 ± 3.0	0.35	
24321.24.....	411.047	24321.24	4.5	0.00	3.5	7.7 ± 0.4	-0.71	
24301.41.....	411.383	25771.52	4.5	1470.10	5.5	6.0 ± 0.3	-0.81	
24287.54.....	411.618	28089.47	6.5	3801.93	7.5	0.39 ± 0.04	-1.85	
24276.88.....	411.798	29362.52	7.5	5085.64	8.5	0.21 ± 0.03	-2.06	
24261.19.....	412.065	30246.77	8.5	5985.58	7.5	3.76 ± 0.26	-0.76	
24242.19.....	412.388	27308.95	6.5	3066.75	5.5	8.6 ± 0.5	-0.51	
24226.96.....	412.647	25877.16	4.5	1650.20	4.5	1.12 ± 0.09	-1.55	
24217.25.....	412.812	28729.74	7.5	4512.50	6.5	0.96 ± 0.06	-1.41	
24191.30.....	413.255	27993.23	8.5	3801.93	7.5	1.76 ± 0.15	-1.09	
24186.62.....	413.335	26772.08	5.5	2585.46	6.5	10.4 ± 0.6	-0.49	
24178.69.....	413.471	27245.45	5.5	3066.75	5.5	2.33 ± 0.20	-1.14	
24175.10.....	413.532	29260.74	7.5	5085.64	8.5	20.8 ± 1.1	-0.07	
24166.77.....	413.675	27233.53	4.5	3066.75	5.5	3.67 ± 0.25	-1.03	
24153.33.....	413.905	26738.79	6.5	2585.46	6.5	0.275 ± 0.021	-2.00	
24121.31.....	414.454	25771.52	4.5	1650.20	4.5	4.07 ± 0.22	-0.98	
24109.27.....	414.661	30094.85	7.5	5985.58	7.5	1.02 ± 0.08	-1.37	
24056.44.....	415.572	24569.77	4.5	513.33	4.5	0.247 ± 0.021	-2.19	
24054.37.....	415.608	25524.47	6.5	1470.10	5.5	40.2 ± 2.2	0.16	

TABLE 3—Continued

Transition Wavenumber (cm ⁻¹)	λ in Air (nm)	Upper Level (cm ⁻¹)	Upper J	Lower Level (cm ⁻¹)	Lower J	Transition Probability (10 ⁶ s ⁻¹)	$\log_{10} gf$	Notes ^a
24053.34.....	415.625	24053.34	4.5	0.00	3.5	3.35 ± 0.19	-1.06	
24028.45.....	416.056	28540.95	7.5	4512.50	6.5	7.6 ± 0.4	-0.50	
24011.16.....	416.356	25481.27	5.5	1470.10	5.5	0.089 ± 0.016	-2.56	
23954.70.....	417.337	24468.03	3.5	513.33	4.5	1.53 ± 0.09	-1.50	
23942.26.....	417.554	27744.19	6.5	3801.93	7.5	2.30 ± 0.15	-1.08	
23941.90.....	417.560	29027.54	8.5	5085.64	8.5	12.2 ± 0.7	-0.24	
23932.05.....	417.732	24445.38	5.5	513.33	4.5	25.2 ± 1.4	-0.10	
23925.14.....	417.853	26991.89	5.5	3066.75	5.5	1.50 ± 0.10	-1.33	
23924.51.....	417.864	25394.62	6.5	1470.10	5.5	2.54 ± 0.14	-1.03	
23919.50.....	417.951	27721.43	6.5	3801.93	7.5	0.88 ± 0.06	-1.49	
23919.10.....	417.958	25389.21	4.5	1470.10	5.5	8.7 ± 0.4	-0.64	
23882.26.....	418.603	25352.37	5.5	1470.10	5.5	1.55 ± 0.09	-1.31	
23860.24.....	418.989	26926.99	4.5	3066.75	5.5	0.126 ± 0.022	-2.48	
23831.06.....	419.502	25481.27	5.5	1650.20	4.5	5.3 ± 0.4	-0.78	
23809.79.....	419.877	27611.72	7.5	3801.93	7.5	0.49 ± 0.04	-1.68	
23807.91.....	419.910	24321.24	4.5	513.33	4.5	1.14 ± 0.08	-1.52	
23773.11.....	420.525	28285.61	5.5	4512.50	6.5	4.25 ± 0.28	-0.87	
23771.25.....	420.558	28856.89	7.5	5085.64	8.5	6.6 ± 0.4	-0.55	
23739.00.....	421.129	25389.21	4.5	1650.20	4.5	5.23 ± 0.27	-0.86	
23715.89.....	421.539	29701.47	6.5	5985.58	7.5	0.385 ± 0.029	-1.84	
23705.33.....	421.727	26772.08	5.5	3066.75	5.5	1.69 ± 0.11	-1.27	
23694.34.....	421.923	26761.10	5.5	3066.75	5.5	0.160 ± 0.017	-2.29	
23692.47.....	421.956	26759.22	4.5	3066.75	5.5	0.93 ± 0.06	-1.60	
23688.63.....	422.025	26274.09	5.5	2585.46	6.5	5.0 ± 0.3	-0.80	
23683.66.....	422.113	28196.15	6.5	4512.50	6.5	2.64 ± 0.15	-1.01	
23672.03.....	422.320	26738.79	6.5	3066.75	5.5	1.43 ± 0.08	-1.27	
23662.89.....	422.484	28748.53	8.5	5085.64	8.5	2.64 ± 0.16	-0.90	
23646.78.....	422.771	27448.71	6.5	3801.93	7.5	8.4 ± 0.5	-0.50	
23645.07.....	422.802	25295.28	3.5	1650.20	4.5	3.19 ± 0.22	-1.16	
23644.10.....	422.819	28729.74	7.5	5085.64	8.5	3.71 ± 0.21	-0.80	
23643.92.....	422.823	27445.85	7.5	3801.93	7.5	0.84 ± 0.06	-1.44	
23625.28.....	423.156	26210.74	6.5	2585.46	6.5	0.230 ± 0.024	-2.06	
23620.75.....	423.237	24134.08	5.5	513.33	4.5	10.5 ± 0.9	-0.47	
23597.02.....	423.663	26182.48	5.5	2585.46	6.5	0.237 ± 0.023	-2.12	
23576.98.....	424.023	28089.47	6.5	4512.50	6.5	0.55 ± 0.04	-1.68	
23540.01.....	424.689	24053.34	4.5	513.33	4.5	0.61 ± 0.04	-1.79	
23537.38.....	424.737	23537.38	4.5	0.00	3.5	22.7 ± 1.2	-0.21	
23488.35.....	425.623	25138.55	3.5	1650.20	4.5	1.79 ± 0.11	-1.41	
23479.93.....	425.776	27992.43	5.5	4512.50	6.5	1.38 ± 0.11	-1.35	
23448.68.....	426.343	29434.26	6.5	5985.58	7.5	4.29 ± 0.30	-0.79	
23446.01.....	426.392	26031.47	7.5	2585.46	6.5	0.59 ± 0.04	-1.59	
23430.65.....	426.671	25080.86	5.5	1650.20	4.5	3.3 ± 0.3	-0.97	
23409.52.....	427.057	23409.52	4.5	0.00	3.5	1.98 ± 0.12	-1.27	
23397.37.....	427.278	23397.37	3.5	0.00	3.5	3.31 ± 0.17	-1.14	
23372.76.....	427.728	24842.87	5.5	1470.10	5.5	0.99 ± 0.07	-1.49	
23364.71.....	427.876	25014.91	5.5	1650.20	4.5	0.165 ± 0.019	-2.27	
23344.63.....	428.244	27146.56	6.5	3801.93	7.5	9.0 ± 0.5	-0.46	
23343.93.....	428.256	23857.26	5.5	513.33	4.5	1.86 ± 0.14	-1.21	
23333.33.....	428.451	28184.97	8.5	5085.64	8.5	13.7 ± 1.0	-0.17	
23275.16.....	429.522	29260.74	7.5	5985.58	7.5	1.00 ± 0.10	-1.36	
23263.64.....	429.734	24913.85	3.5	1650.20	4.5	1.36 ± 0.08	-1.52	
23261.26.....	429.778	26328.02	6.5	3066.75	5.5	3.86 ± 0.24	-0.82	
23256.94.....	429.858	27769.43	5.5	4512.50	6.5	0.325 ± 0.029	-1.97	
23250.94.....	429.969	24721.04	6.5	1470.10	5.5	1.19 ± 0.07	-1.34	
23231.69.....	430.325	27744.19	6.5	4512.50	6.5	0.43 ± 0.04	-1.78	
23229.98.....	430.357	23229.98	4.5	0.00	3.5	43.7 ± 2.3	0.08	
23207.33.....	430.777	26274.09	5.5	3066.75	5.5	3.63 ± 0.27	-0.92	
23192.66.....	431.050	24842.87	5.5	1650.20	4.5	1.12 ± 0.09	-1.42	
23160.33.....	431.651	26227.09	4.5	3066.75	5.5	0.44 ± 0.03	-1.91	
23143.99.....	431.956	26210.74	6.5	3066.75	5.5	0.290 ± 0.026	-1.94	
23110.84.....	432.576	26912.77	7.5	3801.93	7.5	21.2 ± 1.6	-0.02	
23099.66.....	432.785	24569.77	4.5	1470.10	5.5	0.354 ± 0.029	-2.00	
23099.23.....	432.793	27611.72	7.5	4512.50	6.5	8.9 ± 0.5	-0.40	
23064.04.....	433.453	29701.47	6.5	6637.43	7.5	0.43 ± 0.05	-1.77	
23041.96.....	433.869	29027.54	8.5	5985.58	7.5	16.0 ± 1.0	-0.09	

TABLE 3—Continued

Transition Wavenumber (cm ⁻¹)	λ in Air (nm)	Upper Level (cm ⁻¹)	Upper J	Lower Level (cm ⁻¹)	Lower J	Transition Probability (10 ⁶ s ⁻¹)	$\log_{10} gf$	Notes ^a
23024.05.....	434.206	23537.38	4.5	513.33	4.5	2.32 ± 0.16	-1.18	
22975.28.....	435.128	24445.38	5.5	1470.10	5.5	7.2 ± 0.5	-0.61	
22939.01.....	435.816	25524.47	6.5	2585.46	6.5	17.2 ± 1.1	-0.16	
22936.22.....	435.869	27448.71	6.5	4512.50	6.5	2.87 ± 0.20	-0.94	
22933.35.....	435.924	27445.85	7.5	4512.50	6.5	1.37 ± 0.10	-1.20	
22919.56.....	436.186	24569.77	4.5	1650.20	4.5	0.65 ± 0.05	-1.73	
22913.49.....	436.302	28899.07	6.5	5985.58	7.5	0.136 ± 0.016	-2.26	
22907.59.....	436.414	27993.23	8.5	5085.64	8.5	3.13 ± 0.19	-0.79	
22896.19.....	436.631	23409.52	4.5	513.33	4.5	1.57 ± 0.10	-1.35	
22884.04.....	436.863	23397.37	3.5	513.33	4.5	6.8 ± 0.3	-0.81	
22864.98.....	437.227	23378.31	5.5	513.33	4.5	0.65 ± 0.04	-1.65	
22851.14.....	437.492	24321.24	4.5	1470.10	5.5	2.93 ± 0.17	-1.08	
22850.54.....	437.503	22850.54	3.5	0.00	3.5	3.84 ± 0.21	-1.05	
22839.79.....	437.709	27352.29	5.5	4512.50	6.5	1.36 ± 0.10	-1.33	
22810.41.....	438.273	25877.16	4.5	3066.75	5.5	3.16 ± 0.29	-1.04	
22809.16.....	438.297	25394.62	6.5	2585.46	6.5	0.217 ± 0.020	-2.06	
22796.45.....	438.542	27308.95	6.5	4512.50	6.5	0.264 ± 0.026	-1.97	
22795.18.....	438.566	24445.38	5.5	1650.20	4.5	14.6 ± 0.9	-0.30	
22773.11.....	438.991	24243.21	6.5	1470.10	5.5	0.121 ± 0.009	-2.31	
22766.91.....	439.111	25352.37	5.5	2585.46	6.5	1.63 ± 0.10	-1.25	
22762.95.....	439.187	28748.53	8.5	5985.58	7.5	0.102 ± 0.015	-2.27	a
22744.16.....	439.550	28729.74	7.5	5985.58	7.5	1.18 ± 0.08	-1.26	
22742.04.....	439.591	27179.60	4.5	4437.56	5.5	1.26 ± 0.11	-1.44	
22732.95.....	439.767	27245.45	5.5	4512.50	6.5	0.96 ± 0.10	-1.48	
22716.65.....	440.082	23229.98	4.5	513.33	4.5	8.6 ± 0.5	-0.60	
22671.04.....	440.968	24321.24	4.5	1650.20	4.5	0.123 ± 0.011	-2.44	
22663.98.....	441.105	24134.08	5.5	1470.10	5.5	7.2 ± 0.6	-0.60	
22663.71.....	441.110	22663.71	4.5	0.00	3.5	0.83 ± 0.09	-1.62	
22646.64.....	441.443	23159.97	5.5	513.33	4.5	0.74 ± 0.04	-1.59	
22634.07.....	441.688	27146.56	6.5	4512.50	6.5	2.74 ± 0.15	-0.95	
22583.23.....	442.682	24053.34	4.5	1470.10	5.5	0.60 ± 0.04	-1.75	
22577.90.....	442.787	28563.48	6.5	5985.58	7.5	0.39 ± 0.06	-1.79	
22555.37.....	443.229	28540.95	7.5	5985.58	7.5	1.21 ± 0.09	-1.25	
22521.30.....	443.899	23991.40	6.5	1470.10	5.5	1.09 ± 0.07	-1.35	
22495.40.....	444.411	25080.86	5.5	2585.46	6.5	0.264 ± 0.030	-2.03	
22483.88.....	444.638	24134.08	5.5	1650.20	4.5	12.5 ± 1.0	-0.35	
22457.72.....	445.156	25524.47	6.5	3066.75	5.5	28.0 ± 1.7	0.07	
22455.62.....	445.198	22455.62	4.5	0.00	3.5	2.70 ± 0.20	-1.10	
22437.24.....	445.563	30306.15	7.5	7868.91	8.5	1.43 ± 0.12	-1.17	
22433.39.....	445.639	28418.97	8.5	5985.58	7.5	10.4 ± 0.8	-0.25	
22429.45.....	445.717	25014.91	5.5	2585.46	6.5	0.29 ± 0.04	-1.98	
22414.51.....	446.014	25481.27	5.5	3066.75	5.5	0.58 ± 0.05	-1.68	
22403.13.....	446.241	24053.34	4.5	1650.20	4.5	4.08 ± 0.22	-0.91	
22400.27.....	446.298	26912.77	7.5	4512.50	6.5	22.9 ± 1.5	0.04	
22389.84.....	446.506	22389.84	3.5	0.00	3.5	1.84 ± 0.10	-1.36	
22387.15.....	446.559	23857.26	5.5	1470.10	5.5	2.22 ± 0.16	-1.10	
22368.82.....	446.925	28354.40	6.5	5985.58	7.5	4.9 ± 0.3	-0.68	
22360.21.....	447.098	27445.85	7.5	5085.64	8.5	1.17 ± 0.08	-1.25	
22358.06.....	447.140	22358.06	4.5	0.00	3.5	1.24 ± 0.07	-1.43	
22327.86.....	447.745	25394.62	6.5	3066.75	5.5	1.12 ± 0.07	-1.33	
22322.45.....	447.854	25389.21	4.5	3066.75	5.5	0.47 ± 0.03	-1.85	
22285.61.....	448.594	25352.37	5.5	3066.75	5.5	1.00 ± 0.08	-1.44	
22269.83.....	448.912	32464.63	7.5	10194.80	8.5	0.77 ± 0.12	-1.43	
22261.64.....	449.077	28899.07	6.5	6637.43	7.5	1.05 ± 0.08	-1.35	
22259.58.....	449.119	26772.08	5.5	4512.50	6.5	0.38 ± 0.04	-1.86	
22257.41.....	449.163	24842.87	5.5	2585.46	6.5	0.58 ± 0.05	-1.68	
22248.60.....	449.340	26761.10	5.5	4512.50	6.5	2.56 ± 0.17	-1.03	
22229.54.....	449.726	26031.47	7.5	3801.93	7.5	0.85 ± 0.07	-1.38	
22226.29.....	449.791	26738.79	6.5	4512.50	6.5	2.25 ± 0.13	-1.02	
22214.01.....	450.040	31256.77	6.5	9042.76	7.5	0.62 ± 0.08	-1.58	
22208.60.....	450.150	28213.87	3.5	6005.27	4.5	1.47 ± 0.15	-1.45	
22207.05.....	450.181	23857.26	5.5	1650.20	4.5	5.7 ± 0.4	-0.69	
22187.65.....	450.575	22187.65	4.5	0.00	3.5	0.211 ± 0.019	-2.19	
22183.54.....	450.658	22696.87	5.5	513.33	4.5	2.48 ± 0.14	-1.04	
22150.38.....	451.333	22663.71	4.5	513.33	4.5	1.53 ± 0.16	-1.33	

TABLE 3—Continued

Transition Wavenumber (cm ⁻¹)	λ in Air (nm)	Upper Level (cm ⁻¹)	Upper J	Lower Level (cm ⁻¹)	Lower J	Transition Probability (10 ⁶ s ⁻¹)	$\log_{10} gf$	Notes ^a
22135.58.....	451.635	24721.04	6.5	2585.46	6.5	3.92 ± 0.20	-0.77	
22014.10.....	454.127	25080.86	5.5	3066.75	5.5	4.9 ± 0.5	-0.74	
22007.65.....	454.260	27993.23	8.5	5985.58	7.5	9.5 ± 0.5	-0.28	
21994.44.....	454.533	28926.24	4.5	6931.80	5.5	1.28 ± 0.13	-1.40	
21948.16.....	455.491	25014.91	5.5	3066.75	5.5	0.102 ± 0.017	-2.42	
21942.29.....	455.613	22455.62	4.5	513.33	4.5	1.17 ± 0.09	-1.44	
21939.41.....	455.673	23409.52	4.5	1470.10	5.5	1.45 ± 0.08	-1.35	
21926.05.....	455.951	28563.48	6.5	6637.43	7.5	0.73 ± 0.11	-1.49	a
21918.05.....	456.117	21918.05	4.5	0.00	3.5	0.72 ± 0.05	-1.65	
21908.21.....	456.322	23378.31	5.5	1470.10	5.5	3.53 ± 0.18	-0.88	
21887.18.....	456.761	23537.38	4.5	1650.20	4.5	1.58 ± 0.10	-1.31	
21844.73.....	457.648	22358.06	4.5	513.33	4.5	0.168 ± 0.010	-2.28	
21831.21.....	457.931	27816.79	7.5	5985.58	7.5	6.5 ± 0.4	-0.48	
21800.11.....	458.585	27805.38	3.5	6005.27	4.5	0.57 ± 0.07	-1.84	b
21759.31.....	459.445	23409.52	4.5	1650.20	4.5	1.37 ± 0.08	-1.36	
21747.16.....	459.701	23397.37	3.5	1650.20	4.5	2.82 ± 0.15	-1.15	
21698.25.....	460.738	26210.74	6.5	4512.50	6.5	1.76 ± 0.12	-1.10	
21689.87.....	460.916	23159.97	5.5	1470.10	5.5	0.132 ± 0.015	-2.30	
21674.32.....	461.246	22187.65	4.5	513.33	4.5	0.47 ± 0.03	-1.82	
21658.02.....	461.593	30700.78	6.5	9042.76	7.5	0.64 ± 0.08	-1.54	b
21654.29.....	461.673	24721.04	6.5	3066.75	5.5	0.221 ± 0.022	-2.00	
21592.69.....	462.990	25394.62	6.5	3801.93	7.5	0.96 ± 0.07	-1.36	
21579.78.....	463.267	23229.98	4.5	1650.20	4.5	0.94 ± 0.07	-1.52	
21548.62.....	463.937	24134.08	5.5	2585.46	6.5	0.96 ± 0.08	-1.43	
21534.53.....	464.240	29484.61	5.5	7950.08	6.5	1.02 ± 0.10	-1.40	
21518.98.....	464.576	26031.47	7.5	4512.50	6.5	3.35 ± 0.18	-0.76	
21509.77.....	464.775	23159.97	5.5	1650.20	4.5	0.52 ± 0.03	-1.69	
21439.60.....	466.296	25877.16	4.5	4437.56	5.5	0.65 ± 0.07	-1.67	
21404.72.....	467.056	21918.05	4.5	513.33	4.5	1.59 ± 0.09	-1.28	
21254.49.....	470.357	24321.24	4.5	3066.75	5.5	3.05 ± 0.19	-1.00	
21241.07.....	470.654	21241.07	2.5	0.00	3.5	9.8 ± 0.5	-0.71	
21226.76.....	470.972	22696.87	5.5	1470.10	5.5	2.70 ± 0.15	-0.97	
21200.34.....	471.559	22850.54	3.5	1650.20	4.5	4.74 ± 0.25	-0.90	
21160.98.....	472.436	27146.56	6.5	5985.58	7.5	7.9 ± 0.4	-0.43	
21108.06.....	473.620	22578.16	6.5	1470.10	5.5	0.47 ± 0.04	-1.66	
21046.66.....	475.002	22696.87	5.5	1650.20	4.5	0.201 ± 0.018	-2.09	
21013.51.....	475.751	22663.71	4.5	1650.20	4.5	0.223 ± 0.024	-2.12	
20987.98.....	476.330	28856.89	7.5	7868.91	8.5	0.64 ± 0.08	-1.46	
20986.58.....	476.362	24053.34	4.5	3066.75	5.5	1.59 ± 0.09	-1.27	
20985.51.....	476.386	22455.62	4.5	1470.10	5.5	2.45 ± 0.18	-1.08	
20968.77.....	476.766	25481.27	5.5	4512.50	6.5	0.58 ± 0.06	-1.62	
20945.83.....	477.288	26031.47	7.5	5085.64	8.5	1.62 ± 0.13	-1.05	
20924.65.....	477.772	23991.40	6.5	3066.75	5.5	1.26 ± 0.07	-1.22	
20919.11.....	477.898	24721.04	6.5	3801.93	7.5	0.241 ± 0.024	-1.94	
20887.96.....	478.611	22358.06	4.5	1470.10	5.5	1.14 ± 0.07	-1.41	
20839.87.....	479.715	25352.37	5.5	4512.50	6.5	4.92 ± 0.30	-0.69	
20836.10.....	479.802	30002.31	9.5	9166.21	9.5	1.11 ± 0.09	-1.11	
20830.03.....	479.942	20830.03	3.5	0.00	3.5	1.29 ± 0.07	-1.45	
20811.28.....	480.374	27448.71	6.5	6637.43	7.5	0.59 ± 0.06	-1.54	
20753.21.....	481.719	26738.79	6.5	5985.58	7.5	1.07 ± 0.07	-1.28	
20739.63.....	482.034	22389.84	3.5	1650.20	4.5	4.36 ± 0.22	-0.92	
20717.55.....	482.548	22187.65	4.5	1470.10	5.5	10.8 ± 0.5	-0.42	
20694.83.....	483.078	26182.48	5.5	5487.65	6.5	0.27 ± 0.04	-1.95	
20672.57.....	483.598	20672.57	4.5	0.00	3.5	1.42 ± 0.08	-1.30	
20574.51.....	485.903	23159.97	5.5	2585.46	6.5	8.6 ± 0.4	-0.44	
20550.06.....	486.481	28418.97	8.5	7868.91	8.5	1.42 ± 0.13	-1.04	
20502.42.....	487.611	25014.91	5.5	4512.50	6.5	1.36 ± 0.15	-1.23	
20447.95.....	488.910	21918.05	4.5	1470.10	5.5	3.60 ± 0.19	-0.89	
20441.28.....	489.069	24243.21	6.5	3801.93	7.5	7.1 ± 0.4	-0.45	
20393.99.....	490.204	20907.32	5.5	513.33	4.5	1.06 ± 0.06	-1.34	
20342.76.....	491.438	23409.52	4.5	3066.75	5.5	5.47 ± 0.28	-0.70	
20335.53.....	491.613	28285.61	5.5	7950.08	6.5	0.72 ± 0.07	-1.50	
20330.37.....	491.738	24842.87	5.5	4512.50	6.5	0.83 ± 0.06	-1.44	
20316.70.....	492.069	20830.03	3.5	513.33	4.5	8.9 ± 0.5	-0.59	
20311.56.....	492.193	23378.31	5.5	3066.75	5.5	0.078 ± 0.008	-2.47	

TABLE 3—Continued

Transition Wavenumber (cm ⁻¹)	λ in Air (nm)	Upper Level (cm ⁻¹)	Upper J	Lower Level (cm ⁻¹)	Lower J	Transition Probability (10 ⁶ s ⁻¹)	$\log_{10} gf$	Notes ^a
20303.33.....	492.393	31186.58	3.5	10883.25	4.5	1.9 ± 0.3	-1.25	
20283.10.....	492.884	31675.29	8.5	11392.19	9.5	0.95 ± 0.08	-1.21	
20225.16.....	494.296	26210.74	6.5	5985.58	7.5	1.45 ± 0.14	-1.13	
20210.78.....	494.648	30405.58	7.5	10194.80	8.5	0.62 ± 0.07	-1.44	
20208.55.....	494.702	24721.04	6.5	4512.50	6.5	1.46 ± 0.09	-1.13	
20163.23.....	495.814	23229.98	4.5	3066.75	5.5	1.55 ± 0.10	-1.24	
20159.24.....	495.912	20672.57	4.5	513.33	4.5	4.31 ± 0.22	-0.80	
20132.21.....	496.578	24569.77	4.5	4437.56	5.5	0.37 ± 0.04	-1.86	
20126.70.....	496.714	29484.61	5.5	9357.91	5.5	0.67 ± 0.12	-1.53	
20111.41.....	497.091	22696.87	5.5	2585.46	6.5	0.91 ± 0.06	-1.39	
20045.89.....	498.716	26031.47	7.5	5985.58	7.5	2.70 ± 0.16	-0.79	
20036.82.....	498.942	25524.47	6.5	5487.65	6.5	1.24 ± 0.10	-1.19	
20007.82.....	499.665	24445.38	5.5	4437.56	5.5	0.63 ± 0.05	-1.55	
19992.70.....	500.043	22578.16	6.5	2585.46	6.5	0.93 ± 0.05	-1.31	
19947.88.....	501.166	27816.79	7.5	7868.91	8.5	1.71 ± 0.14	-0.99	
19883.68.....	502.785	24321.24	4.5	4437.56	5.5	1.72 ± 0.13	-1.19	
19861.33.....	503.351	29027.54	8.5	9166.21	9.5	4.9 ± 0.4	-0.47	
19742.81.....	506.372	27611.72	7.5	7868.91	8.5	3.87 ± 0.29	-0.62	
19730.72.....	506.683	24243.21	6.5	4512.50	6.5	0.69 ± 0.04	-1.43	
19705.77.....	507.324	28748.53	8.5	9042.76	7.5	0.116 ± 0.022	-2.09	a
19696.52.....	507.562	24134.08	5.5	4437.56	5.5	0.30 ± 0.03	-1.86	
19630.11.....	509.279	22696.87	5.5	3066.75	5.5	5.29 ± 0.27	-0.61	
19582.32.....	510.523	28748.53	8.5	9166.21	9.5	3.48 ± 0.26	-0.61	
19573.31.....	510.757	26210.74	6.5	6637.43	7.5	7.8 ± 0.7	-0.37	
19538.89.....	511.657	25524.47	6.5	5985.58	7.5	0.178 ± 0.022	-2.01	a
19520.72.....	512.133	28563.48	6.5	9042.76	7.5	1.60 ± 0.16	-1.06	
19511.41.....	512.378	22578.16	6.5	3066.75	5.5	4.42 ± 0.22	-0.61	
19485.52.....	513.059	30002.31	9.5	10516.79	10.5	35.4 ± 2.6	0.45	
19478.91.....	513.233	23991.40	6.5	4512.50	6.5	3.49 ± 0.18	-0.71	
19437.22.....	514.334	20907.32	5.5	1470.10	5.5	0.57 ± 0.03	-1.57	b
19409.04.....	515.080	25394.62	6.5	5985.58	7.5	0.321 ± 0.027	-1.75	
19402.21.....	515.262	27352.29	5.5	7950.08	6.5	0.60 ± 0.07	-1.54	
19389.30.....	515.605	30781.49	8.5	11392.19	9.5	2.64 ± 0.21	-0.72	
19355.21.....	516.513	24842.87	5.5	5487.65	6.5	3.8 ± 0.4	-0.74	b
19344.76.....	516.792	23857.26	5.5	4512.50	6.5	1.37 ± 0.13	-1.18	
19311.64.....	517.678	28354.40	6.5	9042.76	7.5	2.59 ± 0.23	-0.84	b
19290.01.....	518.259	25295.28	3.5	6005.27	4.5	3.8 ± 0.3	-0.91	b
19257.12.....	519.144	20907.32	5.5	1650.20	4.5	4.92 ± 0.25	-0.62	b
19252.76.....	519.261	28418.97	8.5	9166.21	9.5	25.4 ± 2.1	0.27	
19179.82.....	521.236	20830.03	3.5	1650.20	4.5	3.40 ± 0.19	-0.96	
19167.71.....	521.565	29362.52	7.5	10194.80	8.5	2.80 ± 0.28	-0.74	
19132.52.....	522.525	31153.86	6.5	12021.34	5.5	0.67 ± 0.12	-1.41	
19120.90.....	522.842	22187.65	4.5	3066.75	5.5	1.28 ± 0.09	-1.28	
19099.82.....	523.419	23537.38	4.5	4437.56	5.5	7.4 ± 0.5	-0.51	
19046.71.....	524.879	28089.47	6.5	9042.76	7.5	0.75 ± 0.09	-1.36	
19043.86.....	524.958	26912.77	7.5	7868.91	8.5	24.2 ± 1.9	0.20	
19039.37.....	525.081	25044.64	3.5	6005.27	4.5	5.7 ± 0.5	-0.72	
19022.37.....	525.551	20672.57	4.5	1650.20	4.5	5.16 ± 0.26	-0.67	
18957.73.....	527.343	24445.38	5.5	5487.65	6.5	13.1 ± 1.0	-0.18	
18887.04.....	529.316	25524.47	6.5	6637.43	7.5	21.2 ± 1.6	0.10	
18854.58.....	530.228	30246.77	8.5	11392.19	9.5	9.6 ± 0.8	-0.14	
18851.30.....	530.320	21918.05	4.5	3066.75	5.5	0.89 ± 0.06	-1.43	
18839.72.....	530.646	25771.52	4.5	6931.80	5.5	2.55 ± 0.21	-0.97	
18827.02.....	531.004	27993.23	8.5	9166.21	9.5	1.37 ± 0.12	-0.98	b
18822.00.....	531.145	26772.08	5.5	7950.08	6.5	7.5 ± 0.6	-0.42	
18811.02.....	531.455	26761.10	5.5	7950.08	6.5	0.92 ± 0.11	-1.33	b
18792.42.....	531.981	23229.98	4.5	4437.56	5.5	17.2 ± 1.3	-0.14	
18774.04.....	532.502	27816.79	7.5	9042.76	7.5	0.39 ± 0.06	-1.58	
18701.43.....	534.570	27744.19	6.5	9042.76	7.5	2.85 ± 0.25	-0.77	
18662.09.....	535.697	28856.89	7.5	10194.80	8.5	7.5 ± 0.7	-0.28	
18647.48.....	536.117	23159.97	5.5	4512.50	6.5	0.64 ± 0.06	-1.48	
18610.12.....	537.193	30002.31	9.5	11392.19	9.5	11.5 ± 1.1	0.00	
18592.67.....	537.697	25524.47	6.5	6931.80	5.5	0.47 ± 0.05	-1.55	
18568.96.....	538.383	27611.72	7.5	9042.76	7.5	0.79 ± 0.09	-1.26	
18553.72.....	538.826	28748.53	8.5	10194.80	8.5	0.66 ± 0.10	-1.29	

TABLE 3—Continued

Transition Wavenumber (cm ⁻¹)	λ in Air (nm)	Upper Level (cm ⁻¹)	Upper J	Lower Level (cm ⁻¹)	Lower J	Transition Probability (10 ⁶ s ⁻¹)	$\log_{10} gf$	Notes ^a
18492.26.....	540.616	29434.26	6.5	10942.00	5.5	2.34 ± 0.30	-0.84	b
18462.76.....	541.480	24468.03	3.5	6005.27	4.5	0.68 ± 0.07	-1.62	
18405.95.....	543.152	27448.71	6.5	9042.76	7.5	5.4 ± 0.5	-0.47	
18403.09.....	543.236	27445.85	7.5	9042.76	7.5	1.04 ± 0.14	-1.13	b
18346.14.....	544.922	28540.95	7.5	10194.80	8.5	2.83 ± 0.29	-0.69	
18324.01.....	545.580	26274.09	5.5	7950.08	6.5	3.4 ± 0.3	-0.75	b
18321.50.....	545.655	30781.49	8.5	12460.00	8.5	2.60 ± 0.25	-0.68	
18260.67.....	547.473	26210.74	6.5	7950.08	6.5	2.19 ± 0.23	-0.86	
18232.41.....	548.322	26182.48	5.5	7950.08	6.5	0.29 ± 0.06	-1.80	
18226.38.....	548.503	28563.48	6.5	10337.10	6.5	1.06 ± 0.14	-1.17	b
18226.15.....	548.510	22663.71	4.5	4437.56	5.5	0.51 ± 0.07	-1.64	
18224.17.....	548.570	28418.97	8.5	10194.80	8.5	9.4 ± 1.0	-0.12	
18219.76.....	548.702	26640.08	3.5	8420.32	4.5	1.72 ± 0.20	-1.21	b
18205.25.....	549.139	32464.63	7.5	14259.38	6.5	0.99 ± 0.20	-1.14	a
18146.73.....	550.910	29088.72	6.5	10942.00	5.5	0.71 ± 0.10	-1.34	
18083.61.....	552.833	24721.04	6.5	6637.43	7.5	0.76 ± 0.06	-1.31	
18065.67.....	553.382	22578.16	6.5	4512.50	6.5	0.91 ± 0.06	-1.23	
18060.78.....	553.532	29434.26	6.5	11373.47	7.5	2.28 ± 0.27	-0.83	b
18018.06.....	554.845	22455.62	4.5	4437.56	5.5	1.16 ± 0.12	-1.27	
18012.74.....	555.008	27921.38	4.5	9908.64	3.5	2.26 ± 0.26	-0.98	
17989.04.....	555.740	29362.52	7.5	11373.47	7.5	2.18 ± 0.28	-0.79	
17920.50.....	557.865	22358.06	4.5	4437.56	5.5	0.33 ± 0.03	-1.81	
17911.07.....	558.159	24842.87	5.5	6931.80	5.5	1.16 ± 0.12	-1.19	b
17890.66.....	558.796	23378.31	5.5	5487.65	6.5	0.39 ± 0.03	-1.66	
17870.01.....	559.442	26912.77	7.5	9042.76	7.5	9.3 ± 0.8	-0.16	
17840.57.....	560.365	20907.32	5.5	3066.75	5.5	0.363 ± 0.023	-1.69	
17791.84.....	561.899	32093.64	7.5	14301.80	8.5	3.0 ± 0.3	-0.65	
17774.99.....	562.432	29484.61	5.5	11709.62	4.5	0.93 ± 0.17	-1.28	a
17770.54.....	562.573	25295.28	3.5	7524.73	3.5	1.99 ± 0.19	-1.12	b
17635.34.....	566.886	29027.54	8.5	11392.19	9.5	5.6 ± 0.5	-0.31	
17574.40.....	568.852	25524.47	6.5	7950.08	6.5	7.3 ± 0.7	-0.31	
17542.32.....	569.892	30002.31	9.5	12460.00	8.5	2.20 ± 0.25	-0.67	
17532.11.....	570.224	23537.38	4.5	6005.27	4.5	2.73 ± 0.21	-0.88	
17519.91.....	570.621	25044.64	3.5	7524.73	3.5	4.1 ± 0.4	-0.80	
17483.42.....	571.812	28856.89	7.5	11373.47	7.5	5.1 ± 0.5	-0.40	
17480.49.....	571.908	21918.05	4.5	4437.56	5.5	0.45 ± 0.04	-1.66	
17456.84.....	572.683	25877.16	4.5	8420.32	4.5	3.1 ± 0.3	-0.81	
17433.32.....	573.455	32581.32	6.5	15148.00	5.5	4.3 ± 0.6	-0.53	
17416.92.....	573.995	27611.72	7.5	10194.80	8.5	1.47 ± 0.17	-0.93	
17414.17.....	574.086	26772.08	5.5	9357.91	5.5	5.0 ± 0.5	-0.53	
17412.92.....	574.127	29434.26	6.5	12021.34	5.5	2.14 ± 0.26	-0.83	b
17410.44.....	574.209	26206.80	3.5	8796.37	2.5	3.7 ± 0.4	-0.83	b
17389.44.....	574.902	24321.24	4.5	6931.80	5.5	0.79 ± 0.08	-1.41	b
17351.20.....	576.169	25771.52	4.5	8420.32	4.5	1.68 ± 0.18	-1.08	
17251.04.....	579.514	27445.85	7.5	10194.80	8.5	0.91 ± 0.11	-1.13	b
17224.71.....	580.400	23229.98	4.5	6005.27	4.5	5.9 ± 0.5	-0.53	
17209.21.....	580.923	22696.87	5.5	5487.65	6.5	0.32 ± 0.06	-1.71	
17202.28.....	581.157	24134.08	5.5	6931.80	5.5	2.27 ± 0.26	-0.86	
17167.47.....	582.336	28540.95	7.5	11373.47	7.5	1.33 ± 0.23	-0.96	
17160.10.....	582.586	25876.54	2.5	8716.45	1.5	7.2 ± 1.0	-0.66	b
17109.18.....	584.320	27992.43	5.5	10883.25	4.5	0.88 ± 0.12	-1.27	a
17067.38.....	585.750	29088.72	6.5	12021.34	5.5	1.55 ± 0.18	-0.95	
17050.43.....	586.333	27992.43	5.5	10942.00	5.5	0.74 ± 0.12	-1.34	a
17008.41.....	587.782	26206.80	3.5	9198.39	3.5	2.05 ± 0.22	-1.07	b
17007.27.....	587.821	30306.15	7.5	13298.88	6.5	0.61 ± 0.09	-1.30	
16852.83.....	593.208	26210.74	6.5	9357.91	5.5	0.35 ± 0.05	-1.59	
16575.67.....	603.127	26912.77	7.5	10337.10	6.5	2.08 ± 0.21	-0.74	
16541.38.....	604.377	32464.63	7.5	15923.26	6.5	1.13 ± 0.23	-1.00	a
16299.52.....	613.345	30781.49	8.5	14481.97	7.5	1.55 ± 0.23	-0.80	
16299.17.....	613.358	31256.77	6.5	14957.60	7.5	1.93 ± 0.29	-0.82	
16166.56.....	618.390	25524.47	6.5	9357.91	5.5	1.48 ± 0.17	-0.92	
16096.88.....	621.066	25295.28	3.5	9198.39	3.5	0.62 ± 0.13	-1.54	b
16012.65.....	624.334	23537.38	4.5	7524.73	3.5	0.35 ± 0.04	-1.69	
16000.00.....	624.827	25877.16	4.5	9877.17	4.5	1.53 ± 0.23	-1.05	
15994.46.....	625.044	25352.37	5.5	9357.91	5.5	0.62 ± 0.08	-1.36	b

TABLE 3—Continued

Transition Wavenumber (cm ⁻¹)	λ in Air (nm)	Upper Level (cm ⁻¹)	Upper J	Lower Level (cm ⁻¹)	Lower J	Transition Probability (10 ⁶ s ⁻¹)	$\log_{10} gf$	Notes ^a
15973.30.....	625.872	26640.08	3.5	10666.78	3.5	2.2 ± 0.3	-0.99	b
15961.86.....	626.320	29260.74	7.5	13298.88	6.5	1.19 ± 0.18	-0.95	b
15925.84.....	627.737	32221.57	7.5	16295.73	8.5	0.66 ± 0.13	-1.21	a
15900.92.....	628.720	24321.24	4.5	8420.32	4.5	0.45 ± 0.05	-1.57	a
15872.63.....	629.841	23397.37	3.5	7524.73	3.5	0.79 ± 0.07	-1.43	b
15854.08.....	630.578	32464.63	7.5	16610.55	8.5	1.24 ± 0.23	-0.93	
15765.07.....	634.138	22696.87	5.5	6931.80	5.5	0.265 ± 0.026	-1.72	a
15731.91.....	635.475	22663.71	4.5	6931.80	5.5	0.23 ± 0.03	-1.87	
15705.25.....	636.554	23229.98	4.5	7524.73	3.5	1.03 ± 0.12	-1.20	
15676.40.....	637.725	28563.48	6.5	12887.08	5.5	1.10 ± 0.18	-1.03	a
15664.58.....	638.206	27245.45	5.5	11580.87	6.5	2.4 ± 0.3	-0.75	
15645.17.....	638.998	27921.38	4.5	12276.21	5.5	2.8 ± 0.4	-0.77	
15611.02.....	640.396	32221.57	7.5	16610.55	8.5	0.83 ± 0.17	-1.09	a
15558.01.....	642.578	28856.89	7.5	13298.88	6.5	1.96 ± 0.27	-0.71	
15540.02.....	643.322	26206.80	3.5	10666.78	3.5	1.46 ± 0.21	-1.14	a
15463.11.....	646.522	32464.63	7.5	17001.53	7.5	3.9 ± 0.6	-0.40	b
15398.52.....	649.233	28285.61	5.5	12887.08	5.5	1.73 ± 0.23	-0.88	
15333.51.....	651.986	31256.77	6.5	15923.26	6.5	2.8 ± 0.4	-0.60	a
15319.56.....	652.580	26206.80	3.5	10887.25	2.5	0.35 ± 0.06	-1.74	a
15191.21.....	658.093	26772.08	5.5	11580.87	6.5	1.83 ± 0.22	-0.85	
15174.88.....	658.802	29434.26	6.5	14259.38	6.5	1.4 ± 0.3	-0.90	b
15064.74.....	663.618	31675.29	8.5	16610.55	8.5	0.97 ± 0.15	-0.94	a
15062.46.....	663.719	26772.08	5.5	11709.62	4.5	1.80 ± 0.23	-0.84	
15060.71.....	663.796	29362.52	7.5	14301.80	8.5	4.5 ± 0.6	-0.32	
15032.28.....	665.052	30781.49	8.5	15749.21	9.5	6.6 ± 0.7	-0.11	
14969.23.....	667.852	27245.45	5.5	12276.21	5.5	0.86 ± 0.13	-1.16	a
14965.62.....	668.014	28563.48	6.5	13597.87	6.5	2.02 ± 0.29	-0.72	
14957.99.....	668.354	23378.31	5.5	8420.32	4.5	0.162 ± 0.019	-1.88	a
14859.83.....	672.769	29484.61	5.5	14624.78	5.5	2.9 ± 0.4	-0.63	
14837.62.....	673.776	27744.19	6.5	12906.57	7.5	2.2 ± 0.3	-0.67	
14812.33.....	674.927	27146.56	6.5	12334.23	6.5	0.76 ± 0.11	-1.14	a
14675.21.....	681.233	27921.38	4.5	13246.17	4.5	1.26 ± 0.25	-1.06	a
14412.60.....	693.646	24321.24	4.5	9908.64	3.5	0.43 ± 0.06	-1.51	a
14408.03.....	693.866	25295.28	3.5	10887.25	2.5	0.84 ± 0.14	-1.32	
14393.32.....	694.575	21918.05	4.5	7524.73	3.5	0.153 ± 0.018	-1.95	a
14020.40.....	713.050	23378.31	5.5	9357.91	5.5	0.157 ± 0.020	-1.84	a
13937.74.....	717.279	22358.06	4.5	8420.32	4.5	0.157 ± 0.028	-1.92	a
13900.40.....	719.206	25481.27	5.5	11580.87	6.5	1.27 ± 0.19	-0.93	
13716.34.....	728.857	21241.07	2.5	7524.73	3.5	0.54 ± 0.07	-1.59	
13309.92.....	751.112	27611.72	7.5	14301.80	8.5	1.49 ± 0.19	-0.70	
13278.32.....	752.900	29027.54	8.5	15749.21	9.5	2.5 ± 0.4	-0.41	a
13041.21.....	766.589	23378.31	5.5	10337.10	6.5	0.114 ± 0.015	-1.92	a
12546.97.....	796.786	22455.62	4.5	9908.64	3.5	0.18 ± 0.03	-1.77	a
12524.63.....	798.207	21241.07	2.5	8716.45	1.5	1.33 ± 0.15	-1.12	
12253.77.....	815.851	27611.72	7.5	15357.96	7.5	0.33 ± 0.06	-1.27	a
12221.88.....	817.980	24243.21	6.5	12021.34	5.5	0.59 ± 0.07	-1.08	b
12033.66.....	830.774	20830.03	3.5	8796.37	2.5	0.78 ± 0.09	-1.19	
11998.56.....	833.204	27146.56	6.5	15148.00	5.5	0.59 ± 0.09	-1.06	a
11908.98.....	839.471	24243.21	6.5	12334.23	6.5	0.27 ± 0.04	-1.39	b
11754.87.....	850.477	22696.87	5.5	10942.00	5.5	0.159 ± 0.021	-1.68	a
11697.50.....	854.648	27993.23	8.5	16295.73	8.5	0.30 ± 0.05	-1.23	
11636.17.....	859.153	22578.16	6.5	10942.00	5.5	0.143 ± 0.017	-1.65	
11590.79.....	862.517	26738.79	6.5	15148.00	5.5	0.23 ± 0.04	-1.45	
11566.24.....	864.348	21241.07	2.5	9674.83	2.5	0.77 ± 0.10	-1.29	
11382.68.....	878.286	27993.23	8.5	16610.55	8.5	0.23 ± 0.04	-1.32	
11356.97.....	880.274	23378.31	5.5	12021.34	5.5	0.039 ± 0.006	-2.27	a
11155.19.....	896.197	20830.03	3.5	9674.83	2.5	0.23 ± 0.03	-1.65	
11030.16.....	906.357	20907.32	5.5	9877.17	4.5	0.069 ± 0.012	-1.99	
10921.38.....	915.384	20830.03	3.5	9908.64	3.5	0.147 ± 0.021	-1.83	a
10434.28.....	958.117	22455.62	4.5	12021.34	5.5	0.067 ± 0.012	-2.03	a

NOTES.—In this table J values are given as decimal numbers (e.g., 3.5) instead of fractions (e.g., 7/2) to facilitate electronic file transfers. Table 3 is also available in machine-readable form in the electronic edition of the *Astrophysical Journal Supplement*.

^a (a) Line appears only on the two highest current spectra. (b) Line has a doublet or triplet structure.

TABLE 4
COMPARISON OF BRANCHING FRACTION FOR Nd II ARRANGED BY UPPER LEVEL

TRANSITION WAVENUMBER (cm ⁻¹)	λ IN AIR (nm)	UPPER LEVEL (cm ⁻¹)	UPPER <i>J</i>	LOWER LEVEL (cm ⁻¹)	LOWER <i>J</i>	BRANCHING FRACTION $\times 100$	
						This Experiment	Maier & Whaling (1977)
23229.98.....	430.357	23229.98	4.5	0.00	3.5	54.7 ± 0.9	61.0
22716.65.....	440.082	23229.98	4.5	513.33	4.5	10.71 ± 0.20	8.8
21579.78.....	463.267	23229.98	4.5	1650.20	4.5	1.18 ± 0.07	1.3
20163.23.....	495.814	23229.98	4.5	3066.75	5.5	1.94 ± 0.08	1.5
18792.42.....	531.981	23229.98	4.5	4437.56	5.5	21.5 ± 1.2	20.2
17224.71.....	580.400	23229.98	4.5	6005.27	4.5	7.4 ± 0.5	6.0
15705.25.....	636.554	23229.98	4.5	7524.73	3.5	1.29 ± 0.13	0.9
24054.37.....	415.608	25524.47	6.5	1470.10	5.5	33.8 ± 0.7	36.7
22939.01.....	435.816	25524.47	6.5	2585.46	6.5	14.4 ± 0.6	16.4
22457.72.....	445.156	25524.47	6.5	3066.75	5.5	23.5 ± 0.8	27.1
20036.82.....	498.942	25524.47	6.5	5487.65	6.5	1.04 ± 0.07	
19538.89.....	511.657	25524.47	6.5	5985.58	7.5	0.149 ± 0.017	
18887.04.....	529.316	25524.47	6.5	6637.43	7.5	17.8 ± 1.0	12.7
18592.67.....	537.697	25524.47	6.5	6931.80	5.5	0.39 ± 0.03	
17574.40.....	568.852	25524.47	6.5	7950.08	6.5	6.1 ± 0.5	6.3
16166.56.....	618.390	25524.47	6.5	9357.91	5.5	1.24 ± 0.13	<0.5
24327.31.....	410.945	26912.77	7.5	2585.46	6.5	39.2 ± 0.8	38.4
23110.84.....	432.576	26912.77	7.5	3801.93	7.5	15.1 ± 0.9	15.9
22400.27.....	446.298	26912.77	7.5	4512.50	6.5	16.2 ± 0.7	18.4
19043.86.....	524.958	26912.77	7.5	7868.91	8.5	17.2 ± 1.1	18.4
17870.01.....	559.442	26912.77	7.5	9042.76	7.5	6.6 ± 0.5	7.2
16575.67.....	603.127	26912.77	7.5	10337.10	6.5	1.48 ± 0.13	1.7
24617.04.....	406.108	28418.97	8.5	3801.93	7.5	55.3 ± 1.0	53.3
23333.33.....	428.451	28418.97	8.5	5085.64	8.5	9.5 ± 0.5	10.3
22433.39.....	445.639	28418.97	8.5	5985.58	7.5	7.2 ± 0.4	7.7
20550.06.....	486.481	28418.97	8.5	7868.91	8.5	0.98 ± 0.08	
19252.76.....	519.261	28418.97	8.5	9166.21	9.5	17.5 ± 1.2	20.0
18224.17.....	548.570	28418.97	8.5	10194.80	8.5	6.5 ± 0.6	6.8
24916.67.....	401.224	30002.31	9.5	5085.64	8.5	72.1 ± 1.0	71.2
20836.10.....	479.802	30002.31	9.5	9166.21	9.5	0.60 ± 0.04	
19485.52.....	513.059	30002.31	9.5	10516.79	10.5	19.1 ± 1.1	20.9
18610.12.....	537.193	30002.31	9.5	11392.19	9.5	6.2 ± 0.5	6.7
17542.31.....	569.892	30002.31	9.5	12460.00	8.5	1.19 ± 0.12	1.1
25877.16.....	386.332	25877.16	4.5	0.00	3.5	16.4 ± 0.6	15.4
25363.83.....	394.151	25877.16	4.5	513.33	4.5	58.3 ± 0.8	60.8
24407.05.....	409.602	25877.16	4.5	1470.10	5.5	0.45 ± 0.05	0.3
24226.96.....	412.647	25877.16	4.5	1650.20	4.5	1.57 ± 0.10	0.9
22810.40.....	438.273	25877.16	4.5	3066.75	5.5	4.5 ± 0.3	4.0
21439.60.....	466.296	25877.16	4.5	4437.56	5.5	0.92 ± 0.08	
17456.84.....	572.683	25877.16	4.5	8420.32	4.5	4.4 ± 0.4	5.6
16000.00.....	624.827	25877.16	4.5	9877.17	4.5	2.2 ± 0.3	
26258.75.....	380.717	26772.08	5.5	513.33	4.5	1.33 ± 0.07	3.7
25301.97.....	395.114	26772.08	5.5	1470.10	5.5	44.0 ± 0.5	45.5
25121.88.....	397.947	26772.08	5.5	1650.20	4.5	18.4 ± 0.3	20.6
24186.62.....	413.335	26772.08	5.5	2585.46	6.5	11.7 ± 0.3	11.2
23705.32.....	421.727	26772.08	5.5	3066.75	5.5	1.89 ± 0.08	1.8
22259.59.....	449.119	26772.08	5.5	4512.50	6.5	0.42 ± 0.04	
18822.01.....	531.145	26772.08	5.5	7950.08	6.5	8.4 ± 0.5	8.6
17414.17.....	574.086	26772.08	5.5	9357.91	5.5	5.6 ± 0.4	5.4
15191.21.....	658.093	26772.08	5.5	11580.87	6.5	2.05 ± 0.23	
15062.46.....	663.719	26772.08	5.5	11709.62	4.5	2.02 ± 0.24	
26271.44.....	380.534	28856.89	7.5	2585.46	6.5	20.0 ± 0.6	39.8
25054.96.....	399.010	28856.89	7.5	3801.93	7.5	46.0 ± 0.7	29.8
24344.40.....	410.656	28856.89	7.5	4512.50	6.5	2.84 ± 0.10	3.9
23771.25.....	420.558	28856.89	7.5	5085.64	8.5	8.5 ± 0.3	10.2
20987.98.....	476.330	28856.89	7.5	7868.91	8.5	0.83 ± 0.10	
18662.09.....	535.697	28856.89	7.5	10194.80	8.5	9.7 ± 0.7	10.6
17483.42.....	571.812	28856.89	7.5	11373.47	7.5	6.6 ± 0.6	5.0
15558.01.....	642.578	28856.89	7.5	13298.88	6.5	2.5 ± 0.3	
26444.84.....	378.038	30246.77	8.5	3801.93	7.5	14.04 ± 0.30	13.4
25161.13.....	397.326	30246.77	8.5	5085.64	8.5	64.9 ± 0.7	60.6
24261.19.....	412.065	30246.77	8.5	5985.58	7.5	4.55 ± 0.22	2.4
18854.58.....	530.228	30246.77	8.5	11392.19	9.5	11.6 ± 0.8	10.9

NOTE.—In this table *J* values are given as decimal numbers (e.g., 3.5) instead of fractions (e.g., 7/2), to facilitate electronic file transfers.

Moore et al. (1966) and the atomic and molecular line lists of Kurucz (e.g., Kurucz 1998 and references therein).³ Almost all Nd II lines that are significantly blended by identified contaminants in the solar spectrum were eliminated, as well as those whose total absorption strengths are probably influenced by lines predicted to occur near them (within about 0.05 Å). We attempted to include as many as possible of the lines used in the Ward et al. (1985) solar Nd analysis. Our completed solar list includes 46 Nd II lines in the wavelength range $3600 \text{ Å} \leq \lambda \leq 5811 \text{ Å}$. These are given in Table 5 along with their excitation potentials and $\log_{10} gf$ values.

For 27 out of the 46 solar lines we derived Nd abundances from equivalent widths (EWs). These were measured with Gaussian line fits and/or direct line profile integrations of the digital version⁴ of the Delbouille et al. (1973) center-of-disk spectrum, employing the interactive software package of Fitzpatrick & Sneden (1987). These EWs are listed in Table 5. The comparison with the EWs measured by Moore et al. (1966) is $\langle \text{EW}_{\text{new}} - \text{EW}_{\text{Moore}} \rangle = -2.2 \pm 0.5 \text{ mÅ}$ ($\sigma = 2.8 \text{ mÅ}$; 26 lines). This is satisfactory, considering that most solar Nd II lines are very weak ($\text{EW} < 5 \text{ mÅ}$), the Moore et al. (1966) measurements were made from tracings of the Minnaert, Mulders, & Houtgast (1940) solar photographic spectral atlas, and most of the offset arises from just a very few lines with large EW discrepancies. The EW comparison with Ward et al. (1985), $\langle \text{EW}_{\text{new}} - \text{EW}_{\text{Ward}} \rangle = -0.3 \pm 0.2 \text{ mÅ}$ ($\sigma = 0.6 \text{ mÅ}$; 8 lines), is much better, probably because their chosen solar spectrum, like ours, was that of Delbouille et al.

Nd abundances for the remaining 19 solar lines were determined from synthetic spectrum matches to the Nd II line and surrounding atomic and molecular features. These lines are designated with “syn” in the solar EW column of Table 5. For both the EW and synthetic spectrum computations, the current version of the LTE line analysis code MOOG (Sneden 1973) was employed. As in previous papers of this series, we adopted the solar model atmosphere of Holweger & Müller (1974), and we assumed a microturbulent velocity of $v_t = 0.85 \text{ km s}^{-1}$. The mean solar photospheric abundance from all 46 lines is $\log \epsilon(\text{Nd}) = 1.45 \pm 0.01$ ($\sigma = 0.05$). The derived Nd abundances show no significant trend with wavelength or EW. There is also no trend with line excitation potential, but the total range is only 1.5 eV, so there is little information in this particular nonvariation.

All solar Nd II lines employed in our study are weak. The strongest ones are 4012.24 Å (EW = 39 mÅ; Moore et al. 1966) and 4156.08 Å (EW = 22.5 mÅ, this study; 30 mÅ, Moore et al.). Other lines are typically at least a factor of 2 weaker than these, and hence mostly fall on the linear part of the curve of growth. Therefore, the derived Nd abundance should be nearly independent of the adopted v_t value, which we confirmed in test calculations that varied v_t by $\pm 0.3 \text{ km s}^{-1}$. The same line weakness renders the Nd II lines insensitive to different assumptions about damping constants. These advantages are partially offset by the increased sensitivity of derived Nd abundances to very weak, possibly unrecognized blends and to continuum placement uncertainties. For this reason, many of the solar lines were analyzed with synthetic

spectra rather than with EW measurements. The derived mean Nd abundance is also somewhat dependent on the choice of model solar atmosphere. With the Kurucz (1998) model, we derived $\log \epsilon(\text{Nd}) = 1.42$; with the Grevesse & Sauval (1998) model, $\log \epsilon(\text{Nd}) = 1.41$. These differences are of the same sign and magnitude as those we previously found for La (Lawler et al. 2001a) and Eu (Lawler et al. 2001c).

We have neglected both hyperfine and isotopic splitting in our abundance analysis. There are seven stable and very long lived isotopes of Nd, whose isotopic percentages in solar system material are ^{142}Nd , 27.13; ^{143}Nd , 12.18; ^{144}Nd , 23.80; ^{145}Nd , 8.30; ^{146}Nd , 17.19; ^{148}Nd , 5.76; and ^{150}Nd , 5.64. The odd isotopes ^{143}Nd and ^{145}Nd have hyperfine splitting, but since they constitute only 20.5% of the total Nd abundance this effect may be ignored. Isotopic splittings vary from line to line, but are always in the range $0.002 \text{ Å} \lesssim \Delta \lambda_{\text{max}} \lesssim 0.004 \text{ Å}$ (Aoki et al. 2001 and references therein). These isotopic shifts produce negligible changes in derived Nd abundances.

Ward et al. (1985) initially derived the photospheric Nd abundance from 23 Nd II lines. They eventually discarded four of those lines because of suspected blending problems and an additional two lines because of uncertainties in branching ratio contributions to the transition probabilities. We attempted to use as many of their lines as possible in our solar Nd analysis. Of their 23 transitions, 5276.88, 5416.38, and 5842.39 Å are not included in the present laboratory analysis; 3990.10 Å is coincident in wavelength with a Ce II line, 4351.28 and 4385.66 Å are compromised by much CH contamination, and 4632.64 and 5431.53 Å are both very weak ($\text{EW} \sim 2 \text{ mÅ}$) and obviously blended. This left 15 lines in common, including four that we employed but Ward et al. eventually discarded. From the 11 lines left standing in both analyses, taking differences in the sense this study minus Ward et al., we derive $\langle \Delta \{\log \epsilon(\text{Nd})\} \rangle = -0.04 \pm 0.03$ ($\sigma = 0.11$), almost identical to the overall difference with the earlier result that we obtained with the complete line list.

Our new solar photospheric abundance, $\log \epsilon(\text{Nd}) = 1.45 \pm 0.01$ ($\sigma = 0.05$), adopting the Holweger & Müller (1974) solar model, is in excellent agreement with the current meteoritic value of 1.46 ± 0.03 (Lodders 2003), and is close to the values of 1.48–1.49 that have been recommended in the various reviews of Grevesse and collaborators (cited above). Thus, Nd may be added to the growing list of rare earth elements whose recent photospheric analyses with new atomic data yield very good agreement with meteoritic data.

4.2. Nd in *r*-Process-rich Stars

One motivation for the present Nd II transition probability study was an attempt to improve the reliability of Nd abundances in *n*-capture-rich metal-poor stars. A sampling of the current literature on such stars (e.g., Westin et al. 2000; Cowan et al. 2002; Hill et al. 2002; Aoki et al. 2001; Sneden et al. 2003) suggests that even when large numbers of Nd II lines are used, the resulting line-to-line abundance scatter is $\sigma \sim 0.2$ dex. This sample standard deviation is poor compared to those of, say, La or Eu, for which the scatter typically is $\sigma \lesssim 0.1$ dex.

To assess the effect of the new *gf*'s on Nd abundances in the *n*-capture-rich stars, we have reanalyzed the spectra of

³ Available at <http://kurucz.harvard.edu>.

⁴ Available at http://mesola.obspm.fr/solar_spect.php.

TABLE 5
EQUIVALENT WIDTHS AND ABUNDANCES FOR FOUR STARS

λ (Å)	EP	$\log_{10} gf$	SUN		CS 22892-052		HD 115444		BD +17°3248	
			EW (mÅ)	$\log \epsilon(\text{Nd})$	EW (mÅ)	$\log \epsilon(\text{Nd})$	EW (mÅ)	$\log \epsilon(\text{Nd})$	EW (mÅ)	$\log \epsilon(\text{Nd})$
3600.90	0.320	-0.86	syn	1.48
3615.81	0.204	-0.76	8.5	-0.35
3665.18	0.204	-0.66	syn	1.44	9.0	-0.01
3738.06	0.559	-0.04	20.0	-0.27
3752.68	0.000	-0.82	syn	1.46
3759.79	0.630	-0.45	5.0	-0.46
3780.38	0.471	-0.35	12.0	-0.34	8.7	-0.06
3784.24	0.380	0.15	31.0	-0.42	9.8	-1.04	22.5	-0.17
3784.84	0.064	-1.04	7.0	-0.40
3810.48	0.742	-0.14	11.5	-0.26
3826.41	0.064	-0.41	23.5	-0.42	7.0	-1.03	14.0	-0.22
3838.98	0.000	-0.24	37.5	-0.36	9.7	-1.12	24.0	-0.18
3887.87	0.064	-0.78	7.5	-0.17
3891.51	0.742	-0.14	6.5	-0.13
3900.22	0.471	0.10	syn	1.42	25.0	-0.42	7.0	-1.07	20.0	-0.10
3927.10	0.182	-0.59	14.0	-0.40
3990.10	0.471	0.13	11.0	-0.90	26.0	0.01
4004.00	0.064	-0.57	18.5	-0.43	12.0	-0.17
4007.43	0.471	-0.40	4.5	1.40
4011.06	0.471	-0.76	3.0	-0.18
4012.24	0.630	0.81	syn	1.48
4012.70	0.000	-0.60	syn	1.47	25.0	-0.31	17.5	-0.02
4013.22	0.182	-1.10	5.5	-0.36	3.5	-0.09
4018.82	0.064	-0.85	syn	1.45	14.0	-0.30	syn	-0.95	7.5	-0.12
4021.33	0.320	-0.10	11.4	1.42	26.5	-0.39	7.2	-1.06	20.0	-0.09
4023.00	0.559	0.04	syn	1.44	syn	-0.34	syn	-0.90	syn	-0.09
4041.06	0.471	-0.53	syn	1.47	9.5	-0.33	5.5	-0.14
4043.59	0.320	-0.71	5.0	-0.17
4051.14	0.380	-0.30	18.5	-0.33	14.0	-0.02
4059.95	0.204	-0.52	5.9	1.39	16.0	-0.40	3.5	-1.11	10.5	-0.14
4061.08	0.471	0.55	52.0	-0.35	20.5	-1.01	42.0	-0.09
4069.26	0.064	-0.57	syn	1.53	24.5	-0.29	syn	-0.87	14.5	-0.09
4109.45	0.320	0.35	21.7	-0.97	49.1	0.07
4133.35	0.320	-0.49	syn	1.50	15.0	-0.34	10.0	-0.08
4135.32	0.630	-0.07	4.5	-0.96	14.5	0.03
4136.75	0.380	-1.03	1.3	1.37
4156.08	0.182	0.16	22.5	1.42
4211.29	0.204	-0.86	5.5	-0.13
4232.37	0.064	-0.47	8.0	-0.98	17.3	-0.12
4284.51	0.630	-0.17	5.5	1.39
4351.28	0.182	-0.61	syn	-0.07
4358.16	0.320	-0.16	9.0	-0.95	20.5	-0.07
4368.63	0.064	-0.81	3.4	-1.06	10.0	-0.08
4385.66	0.204	-0.30	8.0	-1.01	17.8	-0.14
4400.82	0.064	-0.60	4.5	-1.14	11.0	-0.24
4446.38	0.204	-0.35	9.5	1.42	23.0	-0.44	7.2	-1.02	18.0	-0.09
4451.98	0.000	-1.10	2.0	-1.09	7.5	0.00
4462.98	0.559	0.04	syn	1.46	28.5	-0.28	6.0	-1.07	19.5	-0.04
4465.06	0.000	-1.36	4.0	-0.04
4465.59	0.182	-1.10	2.1	1.43	4.0	-0.09
4497.26	0.471	-1.38	0.7	1.50
4501.81	0.204	-0.69	4.1	-0.94	9.0	-0.10
4542.60	0.742	-0.28	6.7	-0.06
4563.22	0.182	-0.88	8.0	0.00
4567.61	0.204	-1.31	1.3	1.44	2.8	-0.03
4645.76	0.559	-0.76	1.9	1.39	4.1	-0.02
4706.54	0.000	-0.71	25.0	-0.32	6.0	-1.02
4709.72	0.182	-0.97	2.1	-1.02
4715.59	0.204	-0.90	4.0	1.52	10.5	-0.34
4763.62	0.380	-1.27	0.9	1.39
4777.72	0.380	-1.22	1.4	1.53
4786.11	0.182	-1.41	1.2	1.46

TABLE 5—Continued

λ (Å)	EP	$\log_{10} gf$	SUN		CS 22892–052		HD 115444		BD +17°3248	
			EW (mÅ)	$\log \epsilon(\text{Nd})$	EW (mÅ)	$\log \epsilon(\text{Nd})$	EW (mÅ)	$\log \epsilon(\text{Nd})$	EW (mÅ)	$\log \epsilon(\text{Nd})$
4797.15	0.559	-0.69	2.6	1.45	1.6	-0.98
4820.34	0.204	-0.92	3.3	-0.85
4825.48	0.182	-0.42	26.0	-0.38	7.0	-1.04	17.5	-0.10
4859.03	0.320	-0.44	16.0	-0.46	5.3	-0.98	13.0	-0.08
4902.04	0.064	-1.34	3.0	-0.16
4914.38	0.380	-0.70	3.2	1.37	9.5	-0.40	2.1	-1.07	6.3	-0.11
4959.12	0.064	-0.80	18.0	-0.36	5.0	-0.97	13.0	-0.02
4987.16	0.742	-0.79	0.8	1.18
5063.72	0.975	-0.62	1.3	1.45	2.2	-0.01
5092.79	0.380	-0.61	syn	1.46	14.5	-0.30	3.5	-0.95	10.0	0.00
5130.59	1.303	0.45	7.0	-0.20
5165.13	0.680	-0.74	3.0	-0.09
5192.61	1.136	0.27	syn	1.43
5212.36	0.204	-0.96	2.5	-0.98	6.7	-0.05
5234.19	0.550	-0.51	4.5	1.48	2.2	-1.07	7.2	-0.08
5249.58	0.975	0.20	syn	1.52	17.0	-0.32	3.0	-1.14	11.5	-0.09
5255.51	0.204	-0.67	5.9	1.43	15.0	-0.45	5.0	-0.96	11.5	-0.09
5273.43	0.680	-0.18	16.0	-0.34
5293.16	0.822	0.10	8.9	1.45	14.5	-0.49	3.3	-1.18	13.0	-0.10
5306.46	0.859	-0.97	0.9	1.50
5311.45	0.985	-0.42	2.0	1.42
5319.81	0.550	-0.14	8.7	1.41	20.5	-0.41	4.1	-1.18	14.2	-0.13
5356.97	1.263	-0.28	1.8	1.45
5371.93	1.411	0.00	2.5	1.45
5485.70	1.263	-0.12	syn	1.50
5698.92	1.544	-0.67	syn	1.47
5740.86	1.159	-0.53	syn	1.56
5811.57	0.859	-0.86	syn	1.53

three stars that we previously studied in detail: HD 115444 (Westin et al. 2000), BD +17°3248 (Cowan et al. 2002), and CS 22892–052 (Sneden et al. 2003). In Table 6 we summarize the previous results for Nd and Eu in these stars, entering also the solar abundances for comparison. The published solar value for Nd is taken from Ward et al. (1985), and that for Eu is taken from Biémont et al. (1982). We re-assessed the abundance of Eu for HD 115444 with the Eu II line data of Lawler et al. (2001c), which were not available when this star was originally analyzed. The

(slightly) adjusted Eu abundance is entered on the “new abundance” line for HD 115444 in Table 6.

We searched the spectra of each star independently for detectable Nd II transitions, and the EW measurements for the chosen lines are entered in Table 5. These newly measured EWs will not be identical to those tabulated in our earlier papers on these stars, but on average the differences are extremely small, typically less than 0.5 mÅ, with a single-line scatter of $\sigma \lesssim 1.0$ mÅ. The large [n-capture/Fe] abundance ratios of these stars allowed us to measure EWs

TABLE 6
MEAN NEODYMIUM ABUNDANCES

Star	$\log \epsilon(\text{Nd}) \pm \sigma$	Number	$\log \epsilon(\text{Eu}) \pm \sigma$	Number	$\log \epsilon(\text{Nd}/\text{Eu})$	Reference
Published Values						
Sun	1.5 ± 0.12	17	0.51 ± 0.08	10	0.99	1, 2
CS 22892–052	-0.27 ± 0.3	52	-0.95 ± 0.03	8	0.68	3
HD 115444	-0.93 ± 0.12	10	-1.63 ± 0.07	5	0.7	4
BD +17°3248	-0.08 ± 0.17	40	-0.67 ± 0.05	9	0.59	5
New Results						
Sun	1.45 ± 0.05	46	0.52 ± 0.04	14	0.93	6
CS 22892–052	-0.37 ± 0.06	37	-0.95 ± 0.03	8	0.58	
HD 115444	-1.02 ± 0.08	37	-1.64 ± 0.02	5	0.62	
BD +17°3248	-0.09 ± 0.06	57	-0.67 ± 0.05	9	0.58	

NOTE.—The new Eu value for HD 115444 is from this paper using gf values from Lawler et al. 2001c.

REFERENCES.—(1) Ward et al. 1985 (solar Nd abundances); (2) Biémont et al. 1982 (solar Eu abundances); (3) Sneden et al. 2003; (4) Westin et al. 2000; (5) Cowan et al. 2002; (6) Lawler et al. 2001c.

cleanly in nearly all cases; synthetic spectrum computations were needed for only a handful of lines. These line lists are fairly conservative, as even more strong Nd II transitions were identified in these stars (especially CS 22892–052). However, those additional lines were blended enough that the effort in creating new synthetic spectrum line lists would not have yielded much additional Nd abundance information.

Applying these Nd II line data with the stellar model atmospheres described in the published analyses yielded the individual line abundances shown in Table 5. The abundance means are given in Table 6. The decrease in line-to-line scatter, σ , is apparent in these tabulations. To further illustrate this, in the top panel of Figure 1 we plot the Nd II line abundances for BD +17°3248 published by Cowan et al. (2002), and in the bottom panel we plot the abundances newly derived in this study. Both the decrease in line-to-line scatter and the lack of a wavelength-dependent abundance signature are clearly seen here.

A similar result with a large decrease in the line-to-line scatter was found for HD 115444 and CS 22892–052. In Figure 2 we plot the Nd II line abundances for the Sun and the three *n*-capture-rich metal-poor stars. Inspection of these data and consideration of the σ values of Table 6 suggests that the dominant sources of line-to-line scatter lie in the solar/stellar analyses of individual Nd II lines rather than in their transition probabilities. First, by far the best spectroscopic data (that is, highest resolving power and

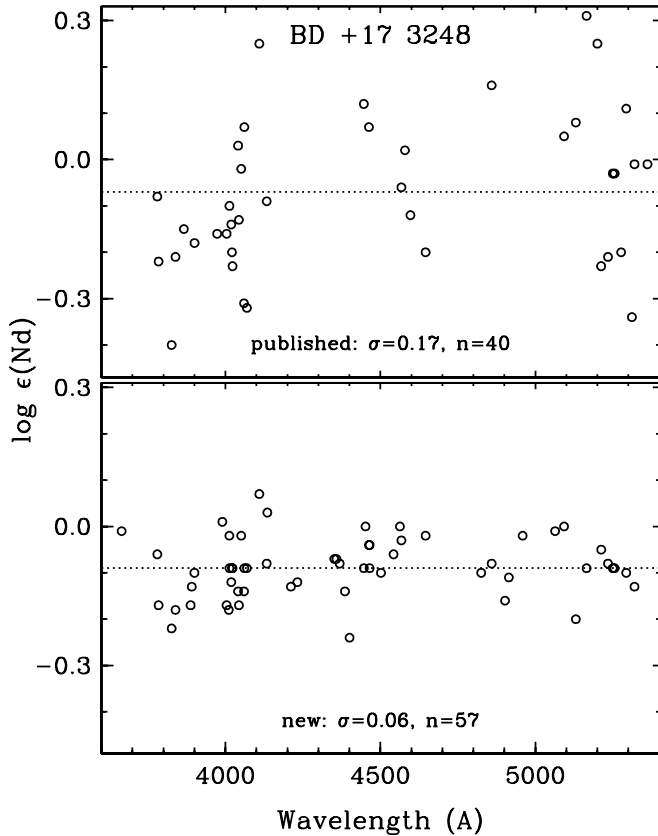


FIG. 1.—Neodymium abundances for BD +17°3248, from individual Nd II lines plotted as a function of wavelength. Top: Published data from Table 2 of Cowan et al. (2002); bottom: the new results. The number of lines employed and the sample standard deviations are indicated in each panel.

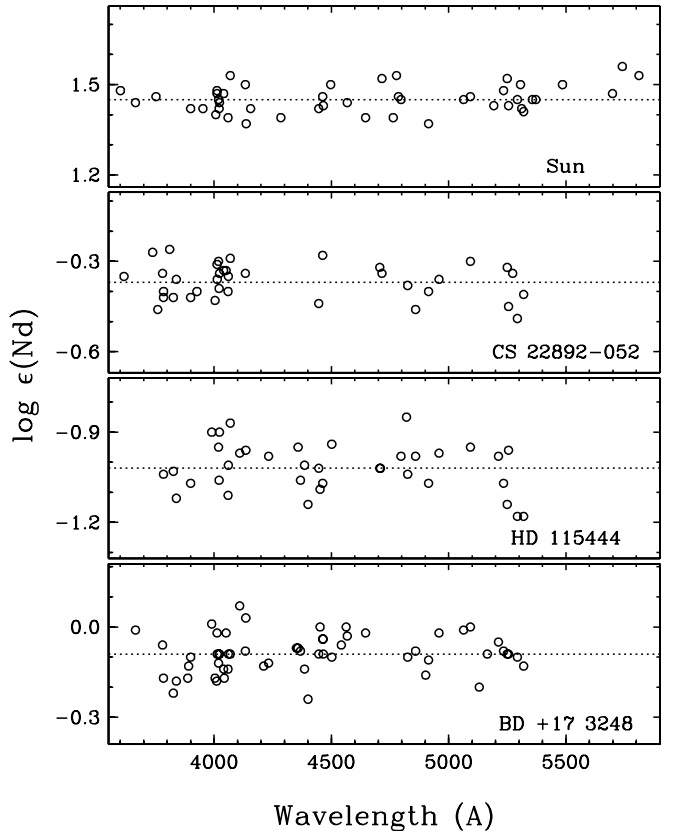


FIG. 2.—Line-by-line Nd abundances as functions of wavelength for the Sun and the three *n*-capture-rich metal-poor giant stars.

S/N) are for the solar photosphere, and we derive the smallest σ value for the solar Nd abundance. Second, the weakest Nd II lines on average are those of HD 115444 (see Table 5), and the line-to-line scatter is largest for that star. Third, there is no obvious pattern to the scatter among the four stars. That is, a given Nd II line does not yield a consistently high or low Nd abundance. This can be quantified by computing the sample standard deviations of the line-by-line differential abundances between any two of the program stars, in the manner described by Westin et al. (2000). Those authors found that the σ values for many species were substantially lower in such a differential abundance analysis between lines measured in the spectra of HD 115444 and another very low metallicity giant, HD 122563. This demonstrated that transition probability uncertainties, which would exactly cancel in differences of abundances for individual lines, were significant contributors to the abundance uncertainties of many elements that they studied. No such effect is seen here. Forming means of the line-by-line differences in the sense $\langle \log[\epsilon(\text{Nd})_{\text{star}}/\epsilon(\text{Nd})_{\text{Sun}}] \rangle$, we find $\sigma = 0.05, 0.09$, and 0.05 , for CS 22892–052, HD 115444, and BD +17°3248, respectively. Furthermore, considering just the three metal-poor giants, and computing differences in the sense $\langle \log[\epsilon(\text{Nd})_{\text{star}}/\epsilon(\text{Nd})_{\text{BD}+17^{\circ}3248}] \rangle$, $\sigma = 0.06$ and 0.08 for CS 22892–052 and HD 115444, respectively. All these differential standard deviations are very similar to those of each star's absolute abundances. They show none of the significant shrinking that would indicate domination of line-to-line uncertainties by the transition probabilities. All these indicators instead point to small-scale (roughly

$\pm 0.02\text{--}0.04$) uncertainties in line measurements (effects of continuum placement, line profile modeling, and blending by other absorbers, known and unidentified).

4.3. Interpretation of the New Nd Abundances

We show in Figure 3 the abundances of the heavy ($Z \geq 56$) n -capture elements in the three metal-poor (i.e., low iron abundance, $[\text{Fe}/\text{H}] < -2$) halo stars, CS 22892–052, BD +17°3248, and HD 115444. The abundances have been relatively scaled in the latter two stars so that the Eu abundances overlap with that of CS 22892–052. It is clear from the figure that in all three stars the newly obtained Nd abundances are remarkably similar. This confirms the results listed in Table 6 where the ratio of $\log \epsilon(\text{Nd/Eu})$ is identical, within error uncertainties, for all three stars. Also shown in Figure 3 are three curves: the total solar system abundances (Lodders 2003), and two solar system r -process elemental curves from Burris et al. (2000) and Arlandini et al. (1999). All three curves are scaled to the Eu abundance of CS 22892–052. It is clear from examining the figure that the elemental abundance distributions in these three stars are not typified by the total solar abundances, but instead match well the predicted r -process-only solar system abundances. Both r -process curves give consistent fits to the newly derived abundance data in all three stars, with some small differences from element to element.

This agreement between the scaled solar r -process abundances and the heavy n -capture abundances in the most metal poor (and oldest) Galactic halo stars has been

reported before (see, e.g., the review by Sneden & Cowan 2003). In solar system material, Nd is produced in approximately equal amounts by the r -process and the s -process (Burris et al. 2000). The s -process is thought to occur in low-mass stars that can take many years to live and die (Busso, Gallino, & Wasserburg 1999). Thus, this slow process could not form elements at early times in the history of the Galaxy, when the metal-poor halo stars first formed. Instead, Nd synthesis at that time must have been dominated by the r -process from rapidly evolving stellar systems, presumably supernovae.

What is different in the current analysis is the precision in the elemental abundances of Nd in the metal-poor stars. This increased precision might allow more refined predictions of the actual solar system r -process abundances. We note that the newly determined stellar Nd abundances, on average, lie between, and might be utilized to further constrain, the r -process predictions of Burris et al. (2000) and Arlandini et al. (1999). In addition, the comparisons shown in Figure 3 are illustrative of the current state of elemental abundance analysis. The tightly constrained abundances for Nd are in contrast to several other elements, for example Sm, that appear to be less precisely determined. Thus, a treatment similar to that done in this paper for Nd might now be warranted for several other nearby elements.

5. SUMMARY

New radiative lifetime measurements, using time-resolved LIF on a slow ion beam, were performed on 168 levels of Nd II. These new measurements are in good agreement with earlier, but much more limited, LIF measurements on Nd II. Branching fractions for more than 700 lines of Nd II were determined from high-resolution emission spectra recorded using the 1 m FTS at the US National Solar Observatory on Kitt Peak. Improved absolute transition probabilities for more than 700 lines of Nd II were determined by combining these lifetime and branching fraction measurements. The solar abundance of Nd has been redetermined with improved accuracy using these transition probabilities, and brought into excellent agreement with the most recent meteoric value. The abundances of Nd in three metal-poor Galactic halo stars, CS 22892–052, BD +17°3248, and HD 115444 have been redetermined with improved accuracy. The ratio $\log \epsilon(\text{Nd/Eu})$ is found to be identical within uncertainties in all three stars, and the elemental abundance distributions of all three stars match the r -process-only solar system abundances. The improving precision and absolute accuracy of elemental abundance determinations in metal-poor Galactic halo stars opens fascinating future possibilities for research on the origins of the chemical elements.

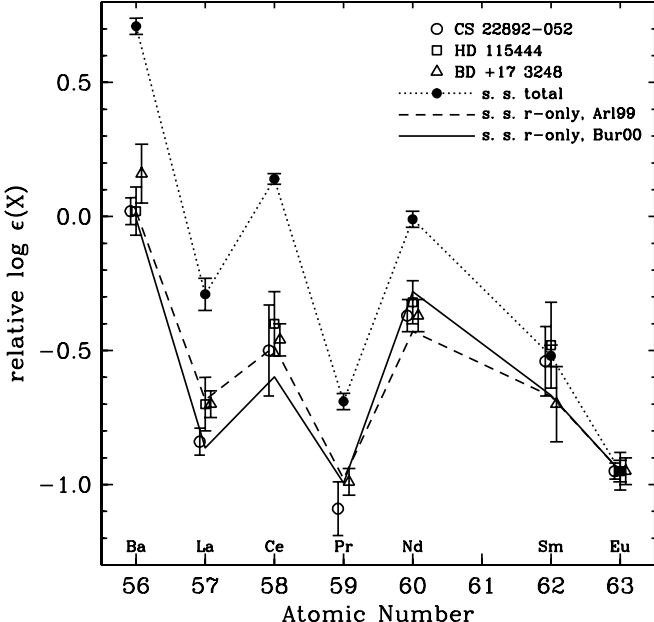


FIG. 3.—Abundances of Ba and the first six stable rare earth elements in the Sun and the three metal-poor giants. The abundance scale for CS 22892–052 is true, and the scales for the other stars have been shifted vertically to force agreement with the Eu abundance of CS 22892–052. The Nd abundances are all from this paper. The other abundances are from: for the Sun, Lodders (2003); for BD +17°3248, Cowan et al. (2002); and for HD 115444, Westin et al. (2000), except for Eu, which is newly determined here. The dotted line is simply to connect the points for the solar abundances. The dashed and solid lines are the r -process solar system abundances of Arlandini et al. (1999) and Burris et al. (2000), respectively, both scaled to force agreement with the Eu abundance of CS 22892–052.

This work is supported by the National Science Foundation under grants AST 02-05124 (J. E. L. and E. A. D. H.), AST 99-87162 (C. S.), and AST 99-86974 (J. J. C.). J. E. Lawler is a guest observer at the National Solar Observatory and he is indebted to Mike Dulick and Detrick Branstrom for help with the 1 m Fourier transform spectrometer. Two Nd spectra from the NSO archives, which were recorded by John Conway during 1983, were used in this study.

REFERENCES

- Adams, D. L., & Whaling, W. 1981, *J. Opt. Soc. Am.*, 71, 1036
- Anders, E., & Grevesse, N. 1989, *Geochim. Cosmochim. Acta*, 53, 197
- Andersen, T., Poulsen, O., Ramanujam, P. S., & Petrakiev Petkov, A. 1975, *Sol. Phys.*, 44, 257
- Aoki, W., Ryan, S. G., Norris, J. E., Beers, T. C., Ando, H., Iwamoto, N., Kajino, T., Mathews, G. J., & Fujimoto, M. Y. 2001, *ApJ*, 561, 346
- Arlandini, C., Käppeler, F., Wisshak, K., Gallino, R., Lugaro, M., Busso, M., & Staniero, O. 1999, *ApJ*, 525, 886
- Biémont, E., Baudoux, M., Kurucz, R. L., Ansbacher, W., & Pinnington, E. H. 1991, *A&A*, 249, 539
- Biémont, E., Karner, C., Meyer, G., Traeger, F., & Zu Putlitz, G. 1982, *A&A*, 107, 166
- Blackwell, D. E., Ibbetson, P. A., Petford, A. D., & Shallis, M. J. 1979a, *MNRAS*, 186, 633
- Blackwell, D. E., Menon, S. L. R., & Petford, A. D. 1984, *MNRAS*, 207, 533
- Blackwell, D. E., Petford, A. D., & Shallis, M. J. 1979b, *MNRAS*, 186, 657
- Blaise, J., Wyart, J. F., Djerad, M. T., & Ahmed, Z. B. 1984, *Phys. Scr.*, 29, 119
- Bord, D. J., Cowley, C. R., & Mirijanian, D. 1998, *Sol. Phys.*, 178, 221
- Burris, D. L., Pilachowski, C. A., Armandroff, T. A., Sneden, C., Cowan, J. J., & Roe, H. 2000, *ApJ*, 544, 302
- Busso, M., Gallino, R., & Wasserburg, G. J. 1999, *ARA&A*, 37, 239
- Corliss, C. H., & Bozman, W. R. 1962, *Experimental Transition Probabilities for Spectral Lines of Seventy Elements* (US NBS Monogr. 53; Washington: GPO)
- Corney, A. 1977, *Atomic and Laser Spectroscopy* (Oxford: Clarendon), 512
- Cowan, J. J., et al. 2002, *ApJ*, 572, 861
- Cowley, C. R., & Corliss, C. H. 1983, *MNRAS*, 203, 651
- Danzmann, K., & Koch, M. 1982, *J. Opt. Soc. Am.*, 72, 1556
- Delbouille, L., Roland, G., & Neven, L. 1973, *Photometric Atlas of the Solar Spectrum from λ 3000 to λ 10000* (Liège: Inst. d'Ap., Univ. de Liège)
- Den Hartog, E. A., Curry, J. J., Wickliffe, M. E., & Lawler, J. E. 1998, *Sol. Phys.*, 178, 239
- Den Hartog, E. A., Fedchak, J. A., & Lawler, J. E. 2001, *J. Opt. Soc. Am. B*, 18, 861
- Den Hartog, E. A., Wickliffe, M. E., & Lawler, J. E. 2002, *ApJS*, 141, 255
- Edlén, B. 1953, *J. Opt. Soc. Am.*, 43, 339
- . 1966, *Metrologia*, 2, 71
- Fedchak, J. A., Den Hartog, E. A., Lawler, J. E., Palmeri, P., Quinet, P., & Biémont, E. 2000, *ApJ*, 542, 1109
- Fitzpatrick, M. J., & Sneden, C. 1987, *BAAS*, 19, 1129
- Gorshkov, V. N., Komarovskii, V. A., Osherovich, A. L., & Penkin, N. P. 1982, *Astrofizika*, 17, 437
- Grevesse, N., & Noels, A. 1993, in *Origin and Evolution of the Elements*, ed. N. Prantzos, E. Vangioni-Flam, & M. Cassé (Cambridge: Cambridge Univ. Press), 15
- Grevesse, N., Noels, A., & Sauval, A. J. 1996, in *ASP Conf. Ser.* 99, Proc. 6th Annual October Astrophysics Conference, ed. S. S. Holt & G. Sonneborn (San Francisco: ASP), 117
- Grevesse, N., & Sauval, A. J. 1998, *Space Sci. Rev.*, 85, 161
- . 2002, *Adv. Space Res.*, 30, 3
- Guo, B., Ansbacher, W., Pinnington, E. H., Ji, Q., & Berends, R. W. 1992, *Phys. Rev. A*, 46, 641
- Hashiguchi, S., & Hasikuni, M. 1985, *J. Phys. Soc. Japan*, 54, 1290
- Hill, V., et al. 2002, *A&A*, 387, 560
- Holweger, H., & Müller, E. A. 1974, *Sol. Phys.*, 39, 19
- Komarovskii, V. A. 1991, *Opt. Spectrosc.*, 71, 559 [trans. in *Opt. Spectrosc. (USSR)* 71, 322]
- Kono, A., & Hattori, S. 1984, *Phys. Rev. A*, 29, 2981
- Kurucz, R. L. 1998, in *IAU Symp.* 189, *Fundamental Stellar Properties: The Interaction between Observation and Theory*, ed T. R. Bedding, A. J. Booth, & J. Davis (Dordrecht: Kluwer), 217
- Lawler, J. E., Bonvallet, G., & Sneden, C. 2001a, *ApJ*, 556, 452
- Lawler, J. E., Wickliffe, M. E., Cowley, C. R., & Sneden, C. 2001b, *ApJS*, 137, 341
- Lawler, J. E., Wickliffe, M. E., Den Hartog, E. A., & Sneden, C. 2001c, *ApJ*, 563, 1075
- Lodders, K. 2003, *ApJ*, 591, 1220
- Maier, R. S., & Whaling, W. 1977, *J. Quant. Spectrosc. Radiat. Transfer*, 18, 501
- Martin, W. C., Zalubas, R., & Hagan, L. 1978, *Atomic Energy Levels: The Rare Earth Elements (NSRDS-NBS 60)* (Washington: GPO), 199
- Meggers, W. F., Corliss, C. H., & Scribner, B. F. 1961, *Tables of Spectral Line Intensities (US NBS Monogr. 32)* (Washington: GPO)
- . 1975, *Tables of Spectral Line Intensities (US NBS Monogr. 145)* (Washington: GPO)
- Minnaert, M. G. J., Mulders, G. F. W., & Houtgast, J. 1940, *Photometric Atlas of the Solar Spectrum* (Amsterdam: D. Schenkel)
- Moore, C. E., Minnaert, M. G. J., & Houtgast, J. 1966, *The Solar Spectrum 2934 Å to 8770 Å (US NBS Monogr. 61)* (Washington: GPO)
- Sneden, C. 1973, *ApJ*, 184, 839
- Sneden, C., & Cowan, J. J. 2003, *Science*, 299, 70
- Sneden, C., et al. 2003, *ApJ*, in press
- Ward, L. 1985, *MNRAS*, 213, 17
- Ward, L., Vogel, O., Arnesen, A., Hallin, R., & Wänström, A. 1985, *Phys. Scr.*, 31, 161
- Wei, S., Fuquan, L., Songmao, W., Peixiong, S., Jianjun, Y., Linggen, S., Jiayong T., & Fujia, Y. 1991, *Phys. Rev. A*, 43, 1451
- Weiss, A. W. 1995, *Phys. Rev. A*, 51, 1067
- Westin, J., Sneden, C., Gustafsson, B., & Cowan, J. J. 2000, *ApJ*, 530, 783
- Whaling, W., Carle, M. T., & Pitt, M. L. 1993, *J. Quant. Spectrosc. Radiat. Transfer*, 50, 7
- Wickliffe, M. E., Lawler, J. E., & Nave, G. 2000, *J. Quant. Spectrosc. Radiat. Transfer*, 66, 363
- Yan, Z.-C., Tambasco, M., & Drake, G. W. F. 1998, *Phys. Rev. A*, 57, 1652